

**AEDC-TR-00-3**



## **Integrated Optical Diagnostics for 16-ft Transonic Wind Tunnel**

Heard Lowry, Mike S. Smith, William T. Bertrand, Fred Heltsley,  
Daryl W. Sinclair, Wim M. Ruyten, and Bryan Hayes  
Sverdrup Technology, Inc., AEDC Group

February 2001

Final Report for Period October 1997 through September 2000

Approved for public release; distribution is unlimited.

**20010405 119**

**ARNOLD ENGINEERING DEVELOPMENT CENTER  
ARNOLD AIR FORCE BASE, TENNESSEE  
AIR FORCE MATERIEL COMMAND  
UNITED STATES AIR FORCE**

## NOTICES

When U. S. Government drawings, specifications, or other data are used for any purpose other than a definitely related Government procurement operation, the Government thereby incurs no responsibility nor any obligation whatsoever, and the fact that the Government may have formulated, furnished, or in any way supplied the said drawings, specifications, or other data, is not to be regarded by implication or otherwise, or in any manner licensing the holder or any other person or corporation, or conveying any rights or permission to manufacture, use, or sell any patented invention that may in any way be related thereto.

Qualified users may obtain copies of this report from the Defense Technical Information Center.

References to named commercial products in this report are not to be considered in any sense as an endorsement of the product by the United States Air Force or the Government.

This report has been reviewed by the Office of Public Affairs (PA) and is releasable to the National Technical Information Service (NTIS). At NTIS, it will be available to the general public, including foreign nations.

## APPROVAL STATEMENT

This report has been reviewed and approved.



KEVIN VLCEK, Major, USAF  
Technology Project Manager  
Applied Technology Division  
Test Operations Directorate

Approved for publication:

FOR THE COMMANDER



ROBERT T. CROOK,  
Deputy Director, Applied Technology Division  
Test Operation Directorate

REPORT DOCUMENTATION PAGE				Form Approved OMB No. 0704-0188							
The public reporting burden for this collection of information is estimated to average 1 hour per response, including the time for reviewing instructions, searching existing data sources, gathering and maintaining the data needed, and completing and reviewing the collection of information. Send comments regarding this burden estimate or any other aspect of this collection of information, including suggestions for reducing the burden, to Department of Defense, Washington Headquarters Services, Directorate for Information Operations and Reports (0704-0188), 1215 Jefferson Davis Highway, Suite 1204, Arlington, VA 22202-4302. Respondents should be aware that notwithstanding any other provision of law, no person shall be subject to any penalty for failing to comply with a collection of information if it does not display a currently valid OMB control number. <b>PLEASE DO NOT RETURN YOUR FORM TO THE ABOVE ADDRESS.</b>											
<b>1. REPORT DATE (DD-MM-YYY)</b> February 2001		<b>2. REPORT TYPE</b> Final Report		<b>3. DATES COVERED (From - To)</b> October 1997 - September 2000							
<b>4. TITLE AND SUBTITLE</b>  Integrated Optical Diagnostics for 16-ft Transonic Wind Tunnel				<b>5a. CONTRACT NUMBER</b>  <b>5b. GRANT NUMBER</b>  <b>5c. PROGRAM ELEMENT NUMBER</b>  <b>5d. PROJECT NUMBER</b>  <b>5e. TASK NUMBER</b>  <b>5f. WORK UNIT NUMBER</b>							
<b>6. AUTHOR(S)</b>  Heard S. Lowry, Mike S. Smith, William T. Bertrand, Fred Heltsley, Daryl W. Sinclair, Wim M. Ruyten, and Bryan Hayes, Sverdrup Technology, Inc., AEDC Group				<b>8. PERFORMING ORGANIZATION REPORT NUMBER</b>  AEDC-TR-00-3							
<b>7. PERFORMING ORGANIZATION NAME(S) AND ADDRESS(ES)</b> Arnold Engineering Development Center/DOS Air Force Materiel Command Arnold Air Force Base, TN 37389-9011				<b>10. SPONSOR/MONITOR'S ACRONYM(S)</b>  <b>11. SPONSOR/MONITOR'S REPORT NUMBER(S)</b>							
<b>9. SPONSORING/MONITORING AGENCY NAME(S) AND ADDRESS(ES)</b> Sponsoring agency: HQ USAF/TE 1650 Air Force Pentagon Washington, DC 20330-1650 Monitoring agency: HQ AFMC/DOR 4375 Chidlaw Rd., S143 Wright-Patterson AFB, OH 45433-5006				<b>12. DISTRIBUTION/AVAILABILITY STATEMENT</b>  Approved for public release; distribution is unlimited.							
<b>13. SUPPLEMENTARY NOTES</b>  Available in Defense Technical Information Center (DTIC)											
<b>14. ABSTRACT</b>  The Integrated Optical Diagnostics project integrated three optical diagnostics systems for use in the Aerodynamic 16-foot transonic wind tunnel testing area. Integration of the systems was provided through an optical diagnostics controller via fiber-optic reflective memory interface hardware. This hardware will be used as the common developmental structure for all future optical diagnostic techniques that will be used in the 16T environment. Control commands and data transfers from the 16T control/data system were accomplished through ethernet connection. This integration will provide aerospace system developers and testers the tools needed to reduce the total time required to conduct a wind tunnel test program.											
<b>15. SUBJECT TERMS</b>  optical diagnostics, integration, wind tunnel, laser vapor screen, boundary-layer transition, Doppler global velocimetry											
<b>16. SECURITY CLASSIFICATION OF:</b> <table border="1" style="width: 100%; border-collapse: collapse;"> <tr> <td style="width: 33%; padding: 2px;">a. REPORT</td> <td style="width: 33%; padding: 2px;">b. ABSTRACT</td> <td style="width: 33%; padding: 2px;">c. THIS PAGE</td> </tr> <tr> <td style="text-align: center;">Unclassified</td> <td style="text-align: center;">Unclassified</td> <td style="text-align: center;">Unclassified</td> </tr> </table>			a. REPORT	b. ABSTRACT	c. THIS PAGE	Unclassified	Unclassified	Unclassified	<b>17. LIMITATION OF ABSTRACT</b>  SAR		<b>18. NUMBER OF PAGES</b>
a. REPORT	b. ABSTRACT	c. THIS PAGE									
Unclassified	Unclassified	Unclassified									
<b>19a. NAMES OF RESPONSIBLE PERSON</b> Maj Kevin Vlcek			<b>19b. TELEPHONE NUMBER (Include area code)</b> (931) 454-4244								

## PREFACE

The work reported herein was conducted by the Arnold Engineering Development Center (AEDC), Air Force Materiel Command (AFMC), under Program Element 65807F, Control Number 6606TS, at the request of HQ USAF/TE. The AEDC project managers were Maj. Bret Indermill, Capt. Phi-Anh Bui, and Capt. Kevin Vlcek. The test results were obtained by Sverdrup Technology, Inc., AEDC Group (a Jacobs Engineering company), support contractor for testing at the AEDC, AFMC, Arnold Air Force Base, Tennessee. The work was performed by Sverdrup Technology, Inc., AEDC Group, during the period from October 1, 1997 through September 30, 2000, under Air Force Job No. 4752.

The authors wish to acknowledge the technical assistance of Dennis Jennings, Ruth Clowers, and Martin Fette (Optical Diagnostic Controller), Davis Rollins and Mary Craig (16T data systems interface), Ric Clippard (Pressure Sensitive Paint and Model Deformation), Ron Porter (Laser Vapor Screen), Courtney Cumberbatch (Shear Stress and Skin Friction), and Don Rotach (instrumentation support). The technical and program assistance of Bret Indermill, Chip Stepanek, and Sid Steeley are also much appreciated.

This manuscript was approved for publication by AEDC STINFO on November 27, 2000.



## CONTENTS

	<u>Page</u>
1.0 INTRODUCTION .....	7
1.1 Requirements .....	7
1.2 Project Vision .....	8
1.3 Overview of Optical Diagnostics .....	9
2.0 OPTICAL DIAGNOSTICS CONTROLLER .....	11
2.1 Hardware Configuration .....	11
2.2 Software Design .....	11
2.3 Capability Description .....	13
2.4 Demonstration Test .....	14
3.0 INTEGRATION OF OPTICAL DIAGNOSTICS .....	15
3.1 Boundary-Layer Transition .....	15
3.2 Doppler Global Velocimetry .....	17
3.3 Laser Vapor Screen .....	21
3.4 Pressure-Sensitive Paint Image Annotation .....	23
3.5 Pressure-Sensitive Paint Model Attitude and Deformation .....	26
3.6 Shear Stress Measurements .....	29
3.7 Multiple Diagnostics Integration Test .....	32
3.8 16T Wind Tunnel Test .....	33
4.0 CONCLUSIONS .....	34
4.1 Summary of Work .....	34
4.2 Recommendations .....	34
REFERENCES .....	35

## ILLUSTRATIONS

### Figure

1. Integrated Optical Diagnostics System .....	37
2. Hardware Configuration of ODC and Optical Diagnostics .....	37
3. ODC Computer System .....	38
4. VMIC Reflective Memory Card .....	38
5. Conceptual Block Diagram of the ODS Software .....	39
6. Hardware Population of ODS .....	39
7. Functional Flow of the ODS Software .....	40
8. Image of ODC Computer Screen .....	40
9. Image of the BLT Computer Screen .....	41
10. Comparison of IR Thermal Imaging and Liquid Crystal Detection Techniques .....	41
11. BLT Camera .....	42
12. LabView <sup>®</sup> Program for Control of BLT Camera from ODC .....	42
13. BLT Data Acquired by BLT Camera and PC .....	43

<u>Figure</u>	<u>Page</u>
14. Transferred BLT Data Displayed on ODC PC.....	43
15. ODC and BLT Computers .....	44
16. BLT Control Panel on the ODC.....	44
17. BLT FITS Playback Display .....	45
18. DGV Setup .....	45
19. DGV Hardware Configuration.....	46
20. Typical Iodine Absorption Spectrum at 20 torr, 80°C.....	46
21. Images of Static Wheel.....	47
22. Frequency Shift versus Piezo Voltage .....	48
23. DGV Measured versus Theoretical Velocity .....	48
24. Images of Rotating Wheel .....	49
25. LabView® Program for Control of DGV Camera from ODC or DGV PC.....	50
26. LabView® Program for Control of DGV Laser from ODC or DGV PC.....	50
27. LabView® Program for Control of DGV System from ODC or DGV PC.....	51
28. WinView Program Displaying DGV Camera Data and Processing .....	51
29. DGV Test Jet with Exhaust Diffuser .....	52
30. Image of Jet Flow .....	52
31. Shadowgraph Image of Jet Flow .....	53
32. DGV Monitors and Control Keyboards .....	53
33. DGV Computer and Control Rack .....	54
34. DGV Remote Laser Controller Screen.....	55
35. Remote Tuning of the DGV Laser Frequency .....	55
36. DGV Remote Energy Monitor .....	56
37. DGV Image Viewer on the ODC .....	56
38. Concept of the LVS Installation.....	57
39. Schematic of the LVS Hardware .....	57
40. Effect of Axial Position .....	58
41. ODC Setup for LVS Integration Demonstration .....	58
42. LVS PC Setup for LVS Integration Demonstration.....	59
43. LVS Laser and Hardware.....	59
44. Screen from Program used for LVS Scan Control from the LVS PC .....	60
45. Screen from Program used for LVS Laser Control from the LVS PC.....	60
46. Screen from Program used for LVS Showtime Control from the LVS PC.....	61
47. Screen from Program used for LVS Scan Control from the ODC PC.....	61
48. Screen from Program used for LVS Laser Control from the ODC PC .....	62
49. Screen from Program used for LVS Showtime Control from the ODC PC .....	62
50. Horizontal Lines Screen.....	63
51. Screen of Lines at 45 deg.....	63
52. Vertical Lines Screen .....	64
53. Vapor Screen Logo.....	64
54. Example of Comparison between PSP Data and CFD Calculations .....	65
55. PSP Image Annotation Demonstration Hardware .....	65
56. Unix Screen of PSP Image Annotation Process.....	66

<u>Figure</u>	<u>Page</u>
57. Schematic of Eight-Camera PSP System for the 16T Wind Tunnel.....	66
58. Circles Indicating Registration Markers Used in Analysis of PSP Images .....	67
59. Yaw Angles from PSP Image Data .....	67
60. Shear Stress Experimental Configuration .....	68
61. Shear Stress Data Images .....	68
62. Shear Stress Data: Hue versus Observation Angle .....	69
63. ODC and BLT Computers .....	69
64. 16T Interface for Data Transfer (Sustainment) .....	70
65. 16T Interface for Data Transfer (Nonsustainment) .....	70
66. BLT Installation in 16T .....	71
67. BLT PC Placement in 16T .....	71
68. LVS Laser Installation in 16T .....	72
69. LVS Controller Installation in 16T .....	72
70. LVS Galvanometer Installed in 16T .....	73
71. LVS PC Setup in 16T .....	73
72. ODC Setup in 16T .....	74
73. BLT 16T CTS Test Data Taken Showing Tunnel Conditions on 7/28/00.....	74
74. BLT 16T CTS Test Data Taken Showing Tunnel Conditions on 7/31/00.....	75

## TABLES

<u>Table</u>	<u>Page</u>
1. Schedule of Deliverables for the ODS Program .....	75

## 1.0 INTRODUCTION

### 1.1 REQUIREMENTS

The purpose of this Test Technology Development and Demonstration (TTD&D) project was to reduce the product definition phase of the aircraft development cycle by applying modern optical instrumentation technology in wind tunnel testing. The need for improved optical instrumentation is described in the 1997 Arnold Engineering Development Center (AEDC) Aircraft Technical Requirements Document (TRD), as follows:

*"Improvements are needed in the ability of wind tunnel test facilities to achieve and maintain test conditions, and in the confidence in data to minimize corrections required. This calls for development of integrated optical diagnostics complementary to computational physics and advanced scientific graphics visualization systems for surface and flow-field measurements."*

Currently, wind tunnel models must be designed and built to internally accommodate hundreds of sensors to measure parameters such as pressure, force, temperature, vibration, and attitude. This makes the model structures complicated and expensive to design and construct. The physical strength required of the model, the size of internal passages needed to route instrumentation cables, and intricate machining requirements demand tradeoffs between the ability to manufacture the model and the ability to acquire data as required. The models often must be dedicated to a single type of test (force and moment, stability and control, jet effects, etc.) with little re-use possible due to different and conflicting instrumentation requirements. Each type of model can cost over a million dollars and can take more than six months to build. Furthermore, the hundreds of channels of instrumentation must be connected and checked for each wind tunnel entry. Complex internal instrumentation also increases the time required to change configurations (e.g., different wing designs) once the model is in the tunnel, thus increasing cost and reducing productivity.

Nonintrusive optical diagnostics techniques can greatly assist our industry partners by allowing the development of test methods that mitigate the need for costly intrusive internal instrumentation. Such techniques will allow industry to build solid models that can be manufactured quickly and cheaply — models that can be modified or reconfigured more easily than those currently in use. The models will be physically stronger, thus reducing model flexure during a test, and they will not require the same level of sophistication to manufacture. Finally, because the optical sensors and integrated optical diagnostic system are part of the test facility rather than the model, the model instrumentation setup time will be greatly reduced.

An integrated system of such optical diagnostics for testing in the AEDC 16-ft Transonic Wind Tunnel (16T) will provide aerospace system developers and testers the tools needed to reduce the total time required to conduct a wind tunnel test program. Such a system will: enable testers to greatly reduce the time and cost required to design and manufacture wind tunnel models; reduce the model assembly time at the test facility; essentially eliminate the model instrumentation setup time; significantly reduce tunnel setup time; and offer the potential to combine multiple wind tunnel tests into a single entry and test run. It will help ensure that AEDC remains a premier

ground test facility for advanced aerospace weapon system development by accurately and economically assessing the performance of aircraft over a wide range of speeds and configurations.

AEDC has been working closely with NASA test centers and industry to develop a coordinated national program for wind tunnel test technologies. This NASA-led effort has identified the critical elements required to make the revolutionary productivity improvements described above. The integrated optical diagnostics system directly satisfies one of the critical elements: institutionalized, advanced instrumentation and test techniques. It enables two others: 1) just-in-time testing processes (e.g., rapid model fabrication), and 2) rapid model installation/removal. It influences three more: 1) rapid data reduction program development, 2) high-speed, real-time data acquisition systems, and 3) overall high facility productivity.

Clearly, the proposed integrated optical diagnostics system has broad military and commercial applications. Such applications have also been recognized by other testing and research centers (e.g., NASA Ames and Langley, Boeing, Deutsche Forschungsanstalt für Luft- und Raumfahrt (DLR), Office National d'Etudes et de Recherches Aerospatiales (ONERA), British Aerospace, Defence Evaluation and Research Agency (DERA), and others).

The products from this TTD&D effort will be directly applied to relevant DoD test programs. AEDC has already performed limited pressure-sensitive paint (PSP) tests for the F-22, F-18E/F, Joint Strike Fighter (JSF), Tier II unmanned vehicle, Theater High-Altitude Air Defense (THAAD) missile, and Extended Expendable Launch Vehicle (EELV) programs. The AIM-9X air-to-air missile program had a very unsatisfactory experience with AEDC's earlier vapor-screen flow visualization method. This led to the development and demonstration of a new prototype system. Other customers have expressed strong interest in full-view PSP capabilities and other advanced test capabilities.

## 1.2 PROJECT VISION

The ultimate vision is that all optical diagnostics be integrated into the 16T environment and that there be immediate display of all final/reduced optically measured test data from any perspective at the console. This would involve making enhanced comparisons of theoretical, computational (CFD, etc.), and experimental optical diagnostic measurements in a time-critical method for test support. An example of this type of work is the automatic image processing required to combine planar laser sheet images into a single, three-dimensional (3-D) image that can be manipulated and animated by the user for scientific graphics visualization. This would require extremely high-speed data acquisition, processing, and display hardware. With the digital optical cameras as the "eyes" of the system, the "brains" of the system would be implemented in sophisticated control and data reduction software designed to combine data/images from eight or more cameras into a single, integrated picture of the airflow on and around the model. A primary focus would be to develop or adapt image-processing techniques to "fuse" multiple data sets and images and to extract as much information as possible about the performance of the vehicle design under test. Data fusion facilitates data measurement certification and model validation, and it improves overall accuracy.

These long-term project objectives are consistent with test and evaluation (T&E) concepts to integrate methodologies for cost effective interactive experimental test results which can be compared with theoretical and computational results. If this ultimate vision is to be achieved, follow-on funding will have to be found.

The practical vision within the scope of the current TTD&D effort was to initiate a methodology whereby mature diagnostics could be prepared for 'plug and play' integration into 16T. This involved emphasizing a methodology for all future diagnostics development that would incorporate the use of a common integration path (via reflective memory connected by fiber optics) between optical diagnostic computers and program system controls to facilitate remote operation. The development of the control and data acquisition systems along this common path will facilitate the integration of these diagnostics into the 16T environment. These diagnostics will also be capable of independent operation at other test sites. The groundwork has been laid to integrate several optical diagnostics systems during the activity of this project. But as these optical diagnostics techniques are improved or upgraded, and as other concepts are introduced, the 'plug and play' methodology must be continued to facilitate integration.

### 1.3 OVERVIEW OF OPTICAL DIAGNOSTICS

The development of optical diagnostics for use in the 16T aerodynamic wind tunnel environment has been pursued at AEDC for many years. Each technique has been documented fairly extensively, but there are as yet no references for the integration of these techniques into the testing arena. The purpose of this document is to provide a better understanding of the development of this integrated optical diagnostic testing environment.

The goal of the integrated Optical Diagnostics System (ODS) was to provide a number of testing enhancements:

- An Optical Diagnostics Controller (ODC) for configuration evaluation and testing of optical diagnostics, and for controlling their operation in the test environment;
- The development of a methodology to integrate detailed images of test configurations with text and graphic annotations;
- The integration of global surface pressure mapping using PSP into the test environment;
- The integration of on-demand global flow-field visualization using Doppler Global Velocimetry (DGV) and Laser Vapor Screen (LVS) techniques into the test environment;
- The integration of a steady-state, six-degree-of-freedom model-position, attitude, and deformation (MAD) measurement capability into the test environment;
- The integration of boundary-layer transition (BLT)/separation detection using infrared (IR) cameras into the test environment;
- The measurement of global surface shear stress vector fields into the test environment.

Eight milestones were scheduled as deliverables for the project:

- M1 Optical Diagnostics Controller
- M2 PSP Image Enhancements for Archives
- M3 Laser-Based Flow Visualization
- M4 Model Deformation and Positioning
- M5 BLT Detection
- M6 Shear Stress and Skin Friction
- M7 DGV Integration
- M8 DGV and BLT Integration

Three demonstrations were scheduled as deliverables:

- D1 Demonstrate PSP Annotation
- D2 Demonstrate ODC Integration in Lab
- D3 Demonstrate Diagnostic Integration in 16T

A project plan revision and a technical report (TR) were also scheduled.

The integrated ODS will consist of scientific-grade digital cameras operating in the infrared and visible range of the spectrum. Visible, IR, and ultraviolet light sources (arc lamps, lasers, photodiodes, etc.) will illuminate the model. On the model's surface, various optical coatings (e.g., PSP) will help to measure the desired surface pressure, temperature, and shear stress sensitivity. For viewing the airflow around the model, a set of adjustable spray nozzles in the wind tunnel stilling chamber will provide the water vapor, particles, or trace gases, which may be needed for flow visualization. An illustration of this integrated environment is shown in Fig. 1.

During the implementation of this project, the suite of optical diagnostics techniques used in 16T was brought to a greater level of maturity. In conjunction with that maturation process, integration into the 16T control and data acquisition environment was developed. The ODC was used to develop comparable operational control software for each of the various diagnostics. The installation and operation of the optical diagnostics techniques in the 16T environment are now greatly simplified, thus reducing the test setup and cycle time. With an integrated suite of diagnostics, the particular optical diagnostics measurements can be optimized to meet the specific test objectives.

In addition to TTD&D funding, AEDC has continued to use internally funded technology or improvement and modernization (I&M) projects (PE65807F) to implement the initial multiview PSP system, reduce uncertainties in PSP data, develop test techniques, increase data acquisition and processing speed, and improve data reporting and analysis tools. AEDC will also continue to cooperate with Wright Laboratories, NASA, industry, and academia to develop advanced instrumentation and test methods.

It is important to note that the successful accomplishment of each of the integration tasks depends in part on the maturity of the diagnostic systems under development. Funding to bring each of these tasks to maturity has been reduced somewhat in previous years. A diagnostic such as shear stress measurement simply is not ready yet (even with sufficient funding) to be integrated under the umbrella of this TTD&D effort. It is expected that advancements from pressure-, temperature-, and shear-sensitive paint research conducted in the future will be included in this integration concept as they develop. An avenue of funding needs to be pursued to accomplish this adaptation of new results and new technologies.

## 2.0 OPTICAL DIAGNOSTICS CONTROLLER

### 2.1 HARDWARE CONFIGURATION

The hardware configuration of the ODC and the optical diagnostics systems is shown in Fig. 2. The host PC is a Dell® Optiplex GX1, running at 350 MHz, with an 8GB hard drive. It is shown in Fig. 3. The operating system is a Microsoft® Windows NT® workstation. An external Jaz® drive provides the backup capability.

The fiber-optic reflective memory interface is a VMICPCI-5588 PCI high-speed (1.2 Gbaud) board with 2-MB onboard memory and a 4-kB FIFO, as shown in Fig. 4. It uses multimode optical fiber cables. Reflective Memory is a high-speed, real-time, deterministic network. With Reflective Memory each node on the network has a local copy of shared data. Writing to Reflective Memory causes the local data on all the nodes to be automatically updated. Reflective Memory allows applications on separate computers to easily share data with little interaction needed from the operating system.

The Reflective Memory Connection is accomplished by connecting the fiber optical cables from each system in a Token Ring Topology. The Token Ring Topology is defined by linking the Transmit (Tx) of one system to the Receive (Rx) of another system until a complete circle is made back to the initial system.

The Ethernet connection to 16T is accomplished by a 100 base T twisted pair Ethernet cable from the ODC to a 16T Network RJ-45 interface jack. The connection is checked by pinging a known IP address on the 16T Network and verifying a response.

### 2.2 SOFTWARE DESIGN

The intent of the ODS software is to provide near real-time (time critical) control and data acquisition of various optical diagnostics from the central ODC. The ODS that will be concurrently controlled from the ODC are the DGV, the LVS, and the BLT systems. The ODC will have a direct connection to the 16T data system through an Ethernet connection to obtain tunnel conditions. The software will allow a user to operate the systems locally, or remotely by using the ODC.



A conceptual block diagram of the ODS software representing the relationships between the various components is shown in Fig. 5. The hardware configuration of the ODS is shown in Fig. 6, along with some of the commercial software components being used in this software development.

The ODS software is divided into four modules. These are the ODC, the Local System User Interface (LSUI), the VMIC Reflective Memory Interface (VRMI), and the Ethernet Interface (EI).

- The ODC will be the central system that can control and collect data from all local systems.
- The LSUI provides a friendly interface to the user of each specific local system. There are three local systems: the DGV, the LVS, and the BLT.
- The VRMI provides an interface to the reflective memory network to all computer systems connected in the ODS.
- The EI provides an interface to the 16T Ethernet connection that will channel tunnel conditions to the ODC.

The ODC computer will communicate with the 16T computer network. This communication will be established over ethernet using TCP/IP. The ODC computer will also access the 16T Analysis and Display System (ADS) test data file using an NFS Link (an NT file system) established prior to the execution of the program.

The programming methods used will comply with Software Development and Maintenance Manual 4500-1. The operating systems will be Microsoft Windows NT 4.0 Workstation for the ODC, DGV, and BLT systems, and Microsoft Windows 2000 Professional® for the LVS system. A majority of the programs will be LabView® v5.1 virtual instruments (vi). C and C++ programming will be used in place of LabView when they are found to be more efficient. Microsoft Visual Basic 6.0® will be used for the LVS. An ANSI C driver and library from VMIC are provided to communicate with reflective memory. National Instruments provides the functions to communicate with the data acquisition (DAQ) boards. The standard TCP/IP protocol will be used for the Ethernet communication to the 16T computers.

A full description of the software development can be found in the following documents:

- Optical Diagnostic System Software Requirements Specification (Document Number: SD-99916-57AT-001)
- Optical Diagnostic System Software Development Plan (Document Number: SD-99916-57AT-002)
- Optical Diagnostic System Software Preliminary Design (Document Number: SD-99916-57AT-003)

- Optical Diagnostic System Software Test Plan (Document Number: SD-99916-57AT-004)
- Optical Diagnostic System Software Detailed Design (Document Number: SD-99916-57AT-005)
- Optical Diagnostic System Software Test Description (Document Number: SD-99916-57AT-006)

## 2.3 CAPABILITY DESCRIPTION

The ODC program and each peripheral system program of the ODS software are interactive, and each has a graphical user interface (GUI). Modules have been developed to control various features of the optical diagnostic systems including:

- DGV Remote Controller
- DGV Remote Energy Monitor
- DGV Remote RS232 Control of CU601 (laser power supply console)
- BLT Control Panel
- BLT FITS Playback Display
- ODC-to-16T Ethernet Interface
- BLT Framegrabber Software
- Remote LVS Player
- LVS Player

It is important to note that the PSP control and data system is a Unix-based system and has previously been integrated into the 16T environment. The ODC thus will have no direct interaction with the PSP system. The minor software changes which were made are discussed in Section 3.4.4.

The general system flow of data and control of the ODS software are shown in Fig. 7. The ODS software communicates with several external pieces of equipment and accesses data on several computers. Communication with each piece of equipment has been isolated to either a unique LabView virtual instrument (vi) or an ANSI C function in a dynamic link library (DLL). The computers in the ODS are connected by fiber optic cable, and each has a VMIC Reflective Memory Card. The ODC, BLT, DGV, and LVS computers are connected in a Token Ring topology.

The ODS software will indicate errors on screen and will try to recover in a predictable and reasonable manner. The program interrupts will occur at the local computer system, ODC (if it is in remote control mode), or in the TCP/IP connection with 16T. The local user of the DGV system can restrict control from the ODC via on-screen controls. If the ODC is controlling remotely, then it can stop a system. If an error has occurred with the 16T communication, then the ODC will send the error to all local computers.

The ODS software will have varying degrees of storage allocation for each computer system. For the DGV system, a minimal allocation for a data file will be assigned. This data file will be in a spreadsheet format and typically should be less than 5 MB. The BLT system will need more storage allocation. Each frame that the BLT infrared camera takes is 150 KB with a 3-KB header. If a user chooses to record 10 frames, then 1,503 KB (1.47 MB) will be needed. If a user records the maximum of 100 frames, then 15,003 KB (14.65 MB) will be needed. The same storage allocation will be needed on the ODC. The ODC will also need storage space for a tunnel conditions file. This file size depends on how many points were taken in a test, but should typically be less than 1 MB. The LVS system needs storage only for Frame files and Show files. These are typically less than 2 MB.

Informal tests and unit tests were used to validate the proper operation of each ODS software unit (i.e., function, subroutine, program, sub vi, or vi). Test programs were used to test each unit individually. The programmer responsible for programming each unit was responsible for the testing.

Informal integration tests were performed to validate the proper operation of the ODS software units when they were integrated into the ODS software. The units from the unit testing process were integrated one at a time for validation. The programmers responsible for programming the different units worked together to complete integrated testing of the software.

Formal tests were developed to validate the proper operation of all ODS software tasks to ensure that all specified requirements were satisfied.

## 2.4 DEMONSTRATION TEST

These various optical diagnostic techniques are interfaced with the 16T control system through the use of reflective memory hardware, which is distributed among the diagnostic PCs. The successful installation and testing of the VMIC boards that are used to implement this network is a crucial part of the effort. The ODC project milestone, M1, is the demonstration of the operation of this computer system and use of the network between the ODC and another diagnostic PC to exchange data.

The demonstration test occurred on July 30, 1999 in Building 676, where the ODC is located. A Windows program was developed to transfer data files from one computer to another over the fiber-optically connected reflective memory network. The PC used for operational control of the BLT Diagnostic System was moved into the lab, and the program was loaded on the BLT and the ODC systems. A 32-MB data file was then successfully transferred through the link. The same file was then copied to another directory to compare the transfer speed. The window showing the transfer program and the performance monitor program of the ODC computer is given in Fig. 8. It is interesting to note that the speed of the network transfer (one reflective - memory read and one disk write) is greater than for the copy (one disk read and one disk write).

The image of the window on the BLT PC shows (in Fig. 9) the verification of the contents of the transferred file. The demonstration shows the successful transfer of data using the ODC and its fiber-optic network.

### **3.0 INTEGRATION OF OPTICAL DIAGNOSTICS**

#### **3.1 BOUNDARY-LAYER TRANSITION**

##### **3.1.1 Requirements**

Nonintrusive test techniques are needed to visualize the state of the boundary layer on "store" models to within a few percent of the characteristic length and to track flow-field streamlines to within 0.25 to 0.5 in. in three orthogonal directions. The nonintrusive measurement of the state of the boundary layer on a store can provide higher quality knowledge from wind tunnel testing than can internal model instrumentation because nonintrusive measurement more closely simulates full-scale flight performance. It provides information for CFD analysts to adjust the boundary-layer state in their codes for comparison with test data, and it contributes to the aircraft customer's requirement for reducing development cycle time. In addition, design changes to correct flow problems early in the development phase will result in a cost saving for the customer. Finally, models of stores tested in the wind tunnel are usually too small to accommodate the extra instrumentation required to measure the state of the boundary layer; therefore, nonintrusive test techniques are needed.

##### **3.1.2 Approach**

Liquid crystal coatings and IR imaging both have been successfully demonstrated for detecting boundary-layer transition and flow separation on wings in production wind tunnels at AEDC (Ref. 1). A comparison of the data from these two techniques is shown in Fig. 10.

The liquid crystal measurement technique depends on changes in shear stress caused by the boundary-layer flow. Cholesteric liquid crystals are sensitive to shear forces and respond quickly enough to allow the acquisition of measurements as fast as test conditions are changed. This can be useful as long as sufficient material remains on the model surface; however, the flow eventually carries it away. This loss mechanism makes the technique somewhat impractical for use in 16T.

For transition detection, it was found that a shallow lighting angle along the span of the wing from near the wingtip with a viewing angle perpendicular to the wing surface gave the best results. This was consistent with results found in the literature (Ref. 2).

Infrared images of a model in a flow field are essentially maps of the surface temperature. Since the rate of mixing in a turbulent boundary layer is greater than that in a laminar boundary layer, the heat-transfer rate in the turbulent boundary layer is greater than that in the laminar

boundary layer. A surface that is initially warmer (cooler) than the freestream manifests a higher (lower) temperature in the presence of a laminar boundary layer as opposed to a turbulent boundary layer. The IR image, which depends on the relative temperature of the surface and the flow, can thus be used to locate the transition between turbulent and laminar boundary layers on the model surface by showing adjacent surface regions with temperatures different enough to be detected. The surface temperature of the model may need to be ramped to provide sufficient data to determine the transition region.

### **3.1.3 Capability Description**

The camera used for the BLT work is an Amber Sentinel model, shown in Fig. 11, which has a spectral response from 8 to 12 microns, a format of  $320 \times 240$  pixels, a frame rate for digital data of about 15 fps. It is controlled by a Dell OptiPlex GX1 350-MHz PC with 64 MB of RAM.

### **3.1.4 Software Design**

The BLT Control Panel is the main control for the remote BLT system. It sets up the system with specified image parameters and can take control when images are acquired. It 1) reads the user-specified parameters and writes them to the reflective memory network for the local system to read; 2) reads a File Image Transfer System (FITS) image file from the reflective memory network and stores it in the specified data directory on the ODC hard drive and notifies the user that it has arrived; and 3) reads an IRIG time file from the reflective memory network, stores it in the same directory as the FITS image file, and then notifies the user that the file has arrived.

The BLT FITS Playback Display program plays back the FITS image file. It displays the image sequence and the corresponding IRIG times. It also displays the 16T tunnel conditions.

The BLT Frame-grabber software was specifically written to take image sequences and the corresponding IRIG time at the BLT computer. This software was modified for integration into the ODS software.

The BLT computer communicates with an infrared camera and an IRIG time generator. An internal ISA framegrabber board is used to communicate with the infrared camera. An internal ISA IRIG decoder board is used to communicate with the IRIG time generator.

### **3.1.5 Integration**

The Labview software routines in the BLT control system that will be used to control the operation of the BLT have been completed. A reflective memory interface has been established between the ODC and the BLT control computer which controls the IR camera that is used to acquire data so that it can be set up and triggered, and data files transferred. The BLT can be operated in either local or remote mode. The VMIC communication software has been expanded to include the code necessary to accomplish these tasks.

The VMIC control software included a module to control the data acquisition camera; it sets the number of frames to acquire, sets the delay between frames, triggers the sequence, and can send the image and IRIG time file immediately after sequence if desired. This activity could be performed by the direction of the ODC as well (interface shown in Fig. 12). The data transfer module reads the FITS image file and displays the sequence acquired from the ODC. It can also set the number of frames to view, set the frame display rate, pause the sequence to look at a still frame, display the associated IRIG time, change color palette, and scale the color range.

The BLT integration project milestone (M5) was accomplished February 24, 2000. The ODC directed the BLT diagnostic system to acquire data from the camera; a sample frame of data from the camera is shown in Fig. 13. The data were then transferred to the ODC and displayed with a simple graphics routine as shown in Fig. 14. The color scale is different for the two images.

The ODC also directed the BLT diagnostic system to acquire data from the BLT camera for the DGV and BLT project milestone (M8). The ODC and BLT computers are shown together in Fig. 15, with the ODC on the right. The software had been upgraded and improved. The control panel window on the ODC is shown in Fig. 16. An example frame of data from this acquisition process is shown in Fig. 17 after being transferred in the FITS format to the ODC. The ODC can transfer images immediately or wait for many frames to be accumulated before the transfer is accomplished.

## **3.2 DOPPLER GLOBAL VELOCIMETRY**

### **3.2.1 Requirements**

Flow diagnostics capabilities in 16T can detect unexpected flow phenomena early in a test program, thus contributing to virtually every aircraft customer's requirement for reducing aircraft development cycle time. Such early detection may save months or years of reconfiguring and repeat testing that could be required if the same flow phenomena were not discovered until later test entries or in flight-test anomalies. An extension of laser vapor-screen flow visualization capabilities available in 16T, Doppler-based velocimetry methods can provide customers with quantitative measurements of off-body flow conditions that will continue to be more useful as aircraft development relies more on computational fluid dynamics (CFD) for flight performance predictions. Further, velocimetry can provide fundamental flow-field information for store drop trajectory prediction and for specialty problems that are growing in importance; examples include acoustic noise-source modification, vortex generation, and aero-optics-based disturbances. What is desired is a nonintrusive flow-field velocimetry system that can characterize aerodynamic flow in near-field and wake regions of wind tunnel models with an initial accuracy target of 10 percent of full scale in velocity.

### **3.2.2 Approach**

DGV is a nonintrusive velocity-measuring technique which uses an iodine vapor cell for a very sharp spectral filter. Light is scattered from a sheet of laser light impinging on an aerosol-

laden (seeded) flow field. Light which is passed through the iodine vapor cell is Doppler-shifted from the original laser frequency by an amount  $\Delta\nu$ , given by  $\Delta\nu = \mathbf{V} \cdot (\hat{o} - \hat{i})/\lambda$ , where  $\mathbf{V}$  is the velocity of the scattering particle,  $\hat{o}$  is the observation direction,  $\hat{i}$  is the incident light direction, and  $\lambda$  is the wavelength of the incident light. The laser source is a pulsed, narrow-bandwidth, frequency-doubled Nd-YAG. The laser is tunable over a frequency range of a few MHz and has a bandwidth of a fraction of one MHz. The laser is tuned to a frequency below or above the absorption transition frequency.

A manually steerable light transmission path for admitting laser energy into the wind tunnel from an external pulsed laser source was developed. A single velocity component, remotely controlled Doppler detection velocimetry camera system was assembled and environmentally hardened for 16T. Demonstration/validation experiments will be performed in Tunnel 16T, subject to a suitable air-on opportunity.

Laboratory experiments should be continued to address remaining issues and to optimize application-related hardware and operating procedures. A flow-seeding system needs to be developed and optimized for global velocimetry in 16T. Data reduction and analysis software should be improved and validated. A three-component global velocimetry system needs eventually to be assembled and demonstrated in 16T.

### 3.2.3 Capability Description

The laser system consists of a Continuum Model NY 82S-10 frequency-doubled Nd:YAG laser, which includes a CW injection seed laser. The seed laser option creates the required narrow-bandwidth output. A piezoelectric mirror mount allows the oscillator cavity length to be changed in very small increments, thus creating a narrow-bandwidth tunable laser system. A dc voltage ranging from  $-10$  to  $+10$  V is applied to the piezoelectric mirror, resulting in a tuning range from approximately  $18788.6 \text{ cm}^{-1}$  to  $18789.7 \text{ cm}^{-1}$  ( $532.238 \text{ nm}$  to  $532.206 \text{ nm}$ ). The oscillator output is processed through two stages of amplification, the preamplifier and the final amplifier, resulting in an output of approximately  $400 \text{ mJ/pulse}$  at a  $10 \text{ Hz}$  rep-rate. A block diagram of the setup is shown in Fig. 18. A picture of the hardware configuration is shown in Fig. 19.

The system is controlled by a Dell Optiplex GX1 350-MHz PC. A 10/100-MHz Ethernet hub connects this computer to two camera controller PCs. These camera systems are used to acquire the reference and test images, which are subsequently subtracted to obtain the velocity fields.

Coarse wavelength identification is accomplished using a Burleigh UV wavemeter, with a resolution of  $0.002 \text{ nm}$ . Fine wavelength identification is accomplished by passing a portion of the laser beam through the iodine cell and then onto a photodiode. The resulting absorption spectrum is recorded using a gated boxcar/integrator system. The laser is tuned to the middle of either the lower or upper side of an iodine absorption transition frequency. If the left edge is chosen, positive velocity components will result in a net increase in signal due to less absorption,

and negative velocity components will result in a net decrease in signal due to more absorption. If the right edge of the transition is used, positive velocity components will result in a net decrease in signal due to more absorption, and negative velocity components will result in a net increase in signal due to less absorption. A typical absorption spectrum is shown in Fig. 20. The transition used for these measurements was the  $18789.28 \text{ cm}^{-1}$  line. This transition was chosen because of its intensity and relative isolation.

Initial verification of the technique was accomplished using a rotating wheel. The wheel rotational velocity was measured using a reflector on the back side, which reflected a helium neon laser beam into a photodiode detector. The frequency of the photodiode pulses was determined, and then the wheel angular velocity and velocity as a function of radius were calculated. The illumination pattern of the motionless wheel as viewed by the camera with the iodine filter is shown in Fig. 21a, and the view of the unfiltered camera is shown in Fig. 21b. The filtered image values were divided by the unfiltered image values, resulting in an image of intensity ratios as shown in Fig. 21c.

An average intensity distribution was calculated, resulting in an intensity ratio corresponding to a particular Doppler shift. This pattern was repeated for several laser wavelengths, creating a Doppler shift versus piezoelectric voltage, which was equivalent to a Doppler shift versus wavelength relationship. This relationship is shown graphically in Fig. 22. For verification purposes, the laser was tuned to the center of the left side (corresponding to a 1.5-V piezoelectric voltage) of the absorption transition. The wheel was then rotated at a rate of 8100 rpm, and using the calibration data, a comparison of the reflective and DGV measurements was accomplished. Tangential velocities were determined using the intensity ratios at various distances from the wheel center. These ratios were then converted to velocities using the calibration data of Fig. 22. The result, along with uncertainties, is shown in Fig. 23. Samples of rotating wheel images are shown in Fig. 24.

### 3.2.4 Software Design

The main control program for the Remote DGV system sets up the laser for a test. It gives the user control of the piezoelectric mirror to allow the user to tune to the desired laser wavelength. It is used to acquire data from the VMIC reflective memory network and to transfer files between the ODC and the local DGV system, and it reads the tunnel conditions from the reflective memory that the ODC has obtained from 16T. The DGV Remote Energy Monitor monitors the laser energy at specified laser pulses while acquiring an image, and it records the data to file.

The DGV Remote Laser Controller program controls the functions of the laser remotely by using reflective memory and the serial port interface (RS232) on the laser. This program also displays the status of the laser.



The DGV Image Viewer is a program that allows a user to see an image taken by the two DGV cameras. The image data format is a Princeton Instruments proprietary format (SPE). This process is only for display of DGV images and does not involve control of the cameras.

The DGV computer communicates with a laser, a National Instruments DAQ card, and cameras. The DGV computer communicates with the laser by a serial port (RS232). The DAQ card is an internal PCI card that comes with LabView drivers for communication. The DGV computer communicates with the cameras over an Ethernet connection and uses third-party software.

### **3.2.5 Integration**

#### **3.2.5.1 Rotating Wheel**

The LabView software routines in the DGV control system that will be used to control the operation of the DGV have been completed. A local network has been established between the DGV control computer and the two-camera controller PCs that are used to acquire and store the data so that these systems can be triggered and data files transferred. The VMIC communication software has been expanded to include the code necessary to accomplish these tasks.

The DGV integration project milestone (M7) and the ODC integration in lab demonstration (D2) were accomplished September 30, 1999. The control software included a module to control the data acquisition cameras (interface shown in Fig. 25); this module initiated the acquisition of data on the two cameras and transferred the data files to the central DGV PC. These functions could be performed by the direction of the ODC as well. The control software also included a laser system control module (interface shown in Fig. 26) which turned the laser on and off, tuned the laser frequency (data shown in Fig. 27), triggered the DGV PC to acquire and transfer data in its normal operational process, and transferred the data to the ODC. Data were acquired on a rotating wheel, as shown in Fig. 28. In this figure, the data from the two cameras are in the smaller windows on the left, and the reduced velocity data reside in the larger window on the right.

#### **3.2.5.2 Jet Test**

The ODC also directed the DGV diagnostic system to acquire data from the DGV system for the DGV and BLT project milestone (M8). In this test, a seeded Mach 2.7 jet was installed to simulate the 16T flow. The seed size needed for successful DGV measurements ranges from 0.2 to 20  $\mu\text{m}$ . A picture of this jet with the exhaust diffuser is shown in Fig. 29. The pressure in the jet can reach up to 1000 psi. A picture of the flow is shown in Fig. 30. A shadowgraph picture of the flow from the jet is shown in Fig. 31.

The two DGV camera monitors and control keyboards are shown in Fig. 32. These are smart terminals that allow access by ODC. The DGV computer and associated control electronics are shown in Fig. 33.

The ODC was used to control the DGV diagnostic system remotely. First, the laser was turned on via the DGV Remote Laser Controller, as shown in Fig. 34, and tuned to the desired laser transition, as shown in Fig. 35. Iodine was introduced manually into the wavelength reference cell and then filled to 100 torr with nitrogen.

Once the cameras were activated for synchronous data acquisition, the next laser pulse initiated the data acquisition sequence for a run. A run consists of images acquired with each camera (three each) which are then averaged together. The laser is shuttered (and unshuttered) upon commands sent from the ODC. The energy of each laser pulse is monitored and shown in a display on the ODC monitor, as shown in Fig. 36. These data are stored so that the pulse can be checked to make sure the bandwidth was sufficiently narrow and to normalize the images to remove variations in the pulse energy. If the laser pulse does not have the correct width, the frames of data taken under this condition must be rejected.

For the dual-integration demonstration, a reference run was first recorded in the absence of flow. A corresponding run was then performed with the flow turned on. Each run was performed under control of the ODC. An example of a false-color data image (scalar velocity in terms of counts) from the camera as viewed on the ODC is shown in Fig. 37.

### **3.3 LASER VAPOR SCREEN**

#### **3.3.1 Requirements**

Tracing of flow-field streamlines, which is rarely attempted outside of a laboratory environment, is required in the wind tunnel to quickly understand the cause of data anomalies. Design changes to correct flow problems early in the development phase will result in a cost saving for the customer.

A nonintrusive, flow visualization system is needed for near-field and wake regions of wind tunnel models with 75 to 90 percent operational reliability for predictable flow visualization scenarios.

#### **3.3.2 Approach**

The vapor-screen technique consists of detecting light scattered from particles in the flow at visible wavelengths (Refs. 3 and 4). The amount of light detected is a function of viewing angle, size, number of particles, and the direction, intensity, and wavelength of the incident light. While most any particle will scatter light, a small particle that will follow the flow, is nondamaging to the model or tunnel, is easy to clean up, and is safe to use is desirable. In Tunnel 16T, global seeding of the flow with water droplets meets these requirements. However, there are some disadvantages in global seeding, including the difficulty in controlling particle size and density, the ability of the air to hold a sufficient amount of moisture, and the absorption of light energy by the water droplets. The best conditions for visualizing the sheet are obtained by operating the tunnel at a humidity condition where the moisture condenses in the near field of the model due to the

temperature drop associated with the acceleration of the flow around the body. If too much moisture is added, the model can become completely obscured by the water droplets (fog effects). The light scattered from the particles in the sheet is detected using still and/or video cameras.

### 3.3.3 Capability Description

The basic concept of the laser-vapor screen installation in the wind tunnel environment is shown in Fig. 38. A galvanometer scanner is used to write a pattern in laser light through the test volume of the 16T tunnel. A camera is used to acquire the visualization data. The system is controlled by a Dell Optiplex GX1 350 MHz PC.

Control of the saturation conditions in the tunnel requires the introduction or removal of a considerable amount of moisture, especially when changes in Mach number and Reynolds number are necessary. In Tunnel 16T, moisture is introduced by injecting steam through a 5-cm-diam line located in the tunnel diffuser. This location was selected for convenience. Moisture is removed by exchanging dry air for moist air. The efficiency of both of these processes is dependent on the moisture content of the replacement air and the saturation conditions for the air in the tunnel.

The location of the cameras depends on the field of view of interest, and on available viewing ports. The particles scatter light more efficiently in the forward direction, but this position is rarely used. It is more common to mount the camera on the model strut, looking upstream along the sting, at nominally 90 deg to the illumination direction. This is more likely to be the view of interest and keeps the camera out of the shadow of the model. Unfortunately, the scattering efficiency of the particles is low in this direction.

The effort to make laser-vapor screen measurements is now an "on demand" capability, requiring only about two days' notice. The current system is also "stand-alone." A schematic of the LVS hardware is shown in Fig. 39. An example of image data as a function of axial position of the laser sheet is shown in Fig. 40.

### 3.3.4 Software Design

The Remote LVS Player is the main remote ODC control program for the LVS system. This program will initialize a laser "show" and then display it. This can be done frame by frame or as an entire "show." The laser display can be manipulated, and the laser display settings can be changed by this program.

The LVS computer communicates with a laser controller computer (QM2000). The QM2000 is a PCI computer board. Control of the QM2000 is established by a third-party DLL.

### 3.3.5 Integration

For the LVS integration, the LVS system was set up in Building 938. The ODC computer is shown in Fig. 41, and the LVS PC was placed on another table as shown in Fig. 42. The LVS laser and its associated hardware are shown in Fig. 43.

The LVS integration project milestone (M3) was accomplished May 31, 2000. The ODC was used to control the LVS diagnostic system remotely. First, the laser was turned on via the LVS Remote Laser Controller, and the chosen "show" pattern displayed on the wall. The control screens of the program for scan control, laser control, and Showtime file selection and initiation, as displayed on the LVS monitor, are shown in Figs. 44, 45, and 46. The corresponding screens from the control program used on the ODC PC are shown in Figs. 47, 48, and 49.

The software used to accomplish the integration included Microsoft® Windows 2000®, Laser-Show Designer 2000, Showtime 2000, and QuadMod 2000 (for the laser computer board). A program was developed to allow the use of reflective memory to control LVS by the ODC. This control software included a laser system control module, which allowed the laser to do the following:

- Turn the laser on and off
- Initialize the laser show
- Display one frame at a time
- Scroll through the frames and display frame as scrolling
- Shutter the laser output
- Rotate frame in X, Y, and Z axes
- Flip frame 90 or -90 deg
- Control the blanking output
- Change X and Y position of frame
- Change X and Y scale of frame
- Open a new frame file and display the frames

Sample display frames are shown in Figs. 50 (horizontal lines), 51 (lines at 45 deg), 52 (vertical lines), and 53 (vapor screen logo).

LVS data are acquired by videorecorder. The tapes are reviewed later and data frames extracted off-line. There is no data acquisition or processing activity that can currently be controlled by the ODC.

## 3.4 PRESSURE-SENSITIVE PAINT (PSP) IMAGE ANNOTATION

### 3.4.1 Requirements

A nonintrusive, full-coverage model surface pressure measurement test technique with 100-percent model view potential and  $\pm 15$ -psf measurement accuracy (stretch goal:  $\pm 10$  psf) is

desired. Such a technique would require only minimal additional installation time as compared to standard pressure taps. Regarding aircraft customers' requirement for reducing aircraft development cycle time, PSP capabilities in Tunnel 16T can provide full surface pressure measurements and force measurements simultaneously, using the same model, thus saving customers the significant cost and schedule time associated with a second model and multiple installation shifts to install and check pressure tap instrumentation. Also, a full-view technique provides the ability to detect, determine, and/or observe unexpected flow phenomena early in the test program. Such early detection could save months or years of reconfiguring and repeat testing that would be required if the same phenomena were not discovered until later test entries or until flight test anomalies developed.

### 3.4.2 Approach

Luminescent paint measurements are assuming an increasingly prominent role in aerodynamic testing (Ref. 5). This is especially true at the AEDC, which has upgraded its PSP system for the 16T wind tunnel to one that employs eight cameras in the test section. To perform PSP measurements, a luminescent coating, whose luminescent yield under suitable illumination is a function of the pressure or temperature at the surface, is applied to a test article. By imaging the surface, it is thus possible to determine the pressure or temperature distribution on the test article. Most importantly, the PSP system is expected to reduce cycle time for test and development projects by providing faster and more comprehensive data than can be obtained by traditional techniques. Model preparation time for PSP measurements essentially consists of painting the wind tunnel model with the appropriate coatings. The coatings have drying times between 30 minutes and 12 hours, compared to the days required for internal instrumentation configuration and setup.

The use of PSP in wind tunnel testing offers the possibility of generating high spatial and temporal resolution model surface pressure maps without the requirement of large numbers of model pressure orifices. Pressure taps and the associated instrumentation often represent a significant fraction of the cost of a wind tunnel model. While pressure taps and thermocouples allow property measurements at discrete locations, a luminescent coating enables measurement of essentially continuous property distributions, limited primarily by the resolution of the imaging equipment. PSP has the potential to simultaneously sample the equivalent of tens of thousands of pressure orifices on a surface in locations such as trailing edges or wingtips, where it is impossible to make measurements with conventional pressure instrumentation. A comparison of PSP data to CFD calculations is shown in Fig. 54.

PSP coatings use the fluorescence process of organic luminophores suspended in a polymeric binder. The photoluminescent probe molecules absorb electromagnetic radiation in a characteristic wavelength range and re-emit a portion of the absorbed energy at a longer wavelength. This re-emission process, usually phosphorescence, depends on the environment of the probe molecule. Specifically, the intensity of the emitted light can be reduced by nonradiative collisional deactivation processes such as occur when the PSP probe molecule interacts with

molecular oxygen. The quenching of the PSP probe luminescence can be quantitatively related to the collision rate (related to the partial pressure) of oxygen at the painted surface that in turn can be related to the surface pressure. Higher surface pressures and thus higher oxygen pressures give rise to lower emission intensities.

### 3.4.3 Capability Description

A basic PSP data acquisition system consists of a model coated with the special PSP paint, a light source to stimulate the material, and image recording and processing hardware. AEDC has already started implementing a multiview PSP system under internal funding. This system consists of: 24 ultraviolet light sources; eight scientific grade digital cameras (16 bit and  $1024 \times 1024$  array resolutions); a six-processor workstation; data storage units; appropriate hardware for mounting, cooling, and electrical power; and data reduction software. The PSP system will be the heart of the integrated optical diagnostics system, and the intent is to build on the PSP cameras and computer to extend it to other wind tunnel measurements.

The first step will be to use the PSP system for test documentation. It is normal practice to take photographs of the various model configurations. Currently film cameras and videotapes are used for this purpose. With proper software changes, the film and video cameras can be eliminated and the PSP cameras used to annotate the images. Eventually, it may be possible to use the PSP system for off-body flow visualization using AEDC's laser vapor-screen technique (see Section 3.3).

The PSP data acquisition system is a UNIX-based system that is very mature and already integrated into the 16T test control system. In addition to the standard use of the PSP system to provide pressure measurements on the surface of a test article, it can also be used for test documentation. It is normal practice to take photographs of the various model configurations. Currently, film cameras and videotapes are used. The objective of the PSP image enhancement and annotation work is to provide a means of documenting more completely similar individual images taken with the PSP cameras.

The software which controls the standard data acquisition and storage of PSP data from the eight-camera system is denoted as PSPDAS. This is run from a Silicon Graphics workstation with the name "davinci."

### 3.4.4 Image Annotation

A development system was established to make the necessary modifications in the PSPDAS software for the image annotation work. This is also a Silicon Graphics workstation, and it has been given the name "rembrandt." A software module has been written (using C++) and tested which allows the insertion of a 256-character description of the image (along with other test information) into a file which is stored in an ORACLE database. The interface between the C++ and ORACLE was programmed using JAVA code. ORACLE was selected because the PSP

annotation information, in addition to other PSP image parameters currently stored on the acquisition system in an Image Database (IDB) file, will be inserted into the Integrated Test Information Systems (ITIS) system, which is based on ORACLE.

The IDB file contains information necessary to process the camera images into a surface map. The addition of the IDB values to the ORACLE database represents the accomplishment of a "stretch goal" in this part of the effort. ORACLE licenses have been acquired for both the davinci and rembrandt systems. ORACLE was chosen to provide compatibility with the AEDC ITIS system so that the annotated images can be examined by querying the ITIS database.

The image enhancement and annotation process has been successfully demonstrated on the developmental system (rembrandt). The software module has also been transferred to the PSPDAS on the davinci system. On September 30, 1999, a demonstration (D1) of the PSP annotation system was performed. A camera was connected to the PSP system (see Fig. 55), and a picture (of an arbitrary scene) was captured and annotated with the modified PSPDAS software. The image and annotations were stored in an ORACLE database on rembrandt. This simulated the storage of data on the ITIS system, which is not kept running continuously at this time. The image annotation function was demonstrated in both the laboratory and test modes of PSPDAS. Test parameters including the time and the annotation supplied by the user were recorded along with the image. A capture of the screen showing the camera image and the dialog box used to input the annotation data is shown in Fig. 56.

### **3.5 PRESSURE-SENSITIVE PAINT MODEL ATTITUDE AND DEFORMATION**

#### **3.5.1 Requirements**

Nonintrusive test article attitude and deformation measurement capabilities at AEDC can provide accurate measurement of aircraft angles of attack and yaw, store position relative to parent aircraft, and wing deflection and deformation. These test techniques are needed to measure the position of a model to within 0.005 to 0.01 in., and deformation of test article surfaces (wing, etc.) to within 0.005 to 0.02 in. There is great interest in accurate position measurements and model control of store trajectories. Models of stores tested in the wind tunnel are usually too small to accommodate the extra instrumentation required to accurately determine model position.

The feasibility of measuring the position of an aircraft model with a photographic technique that uses single or multiple CCD cameras has been demonstrated in Tunnel 16T. The use of the technique to determine the uncertainty in measuring the 6-DOF position of a store is planned. Automation of the image processing to reduce the time required to obtain final position information is also being planned.

### 3.5.2 Approach

#### 3.5.2.1 OPTOTRAK®

At the beginning of this effort, an optical diagnostic system with the trade name OPTOTRAK® was being evaluated for its ability to measure the deformation and position of a test article in the wind tunnel environment. This development uses actively controlled targets in the model and has not been as successful as was desired. The OPTOTRAK system has been tested and is currently being modified by the vendor to try to improve its operation.

The OPTOTRAK system met the quoted accuracy with single degree of freedom (i.e., pitch only) model movement, but not with multiple degree of freedom model movements (i.e., pitch coupled with yaw, etc.). The problem is believed to be in the calculation of the transformation matrix, and the manufacturer (Northern Digital) is working on the problem.

An analysis of linear and angular position measurement accuracy that can be theoretically provided by OPTOTRAK is currently under way.

The next generation of OPTOTRAK needs to eliminate the requirement of installing actively controlled targets in a model. The use of passive targets (or no targets) would greatly reduce installation time as well as enable measurements on smaller models that do not have much room for internal instrumentation cables.

#### 3.5.2.2 PSP

PSP measurements are assuming an increasingly prominent role in aerodynamic testing. AEDC has upgraded its PSP system for the 16-ft Transonic Wind Tunnel to one that will employ eight cameras in the test section, as is shown in Fig. 57. In this technique, a luminescent coating, whose response under suitable illumination is a function of the pressure or temperature at the surface, is applied to a test article. By imaging the surface with a spectrally filtered camera, it is possible to determine the pressure or temperature distribution on the test article.

An important part of the PSP test methodology is the process of mapping two-dimensional (2-D) image data onto a 3-D grid of the test article. To accomplish this task, registration markers are placed on the test article. This presents the interesting opportunity of using the image coordinates of the registration markers to calculate the position and attitude (P&A) of the test article from the optical data acquired by the PSP cameras. By contrast, traditional measurements of model attitude involve a complex procedure for combining and calibrating data from sting-mounted balance sensors and strain gages. The accuracy of such measurements is estimated to be in the range 0.02 to 0.05 deg. The possibility of using the optical data system to improve these accuracies to 0.01 deg or better was investigated to try to meet the level of accuracy desired more and more frequently by AEDC test customers.



### 3.5.3 Capability Description (PSP)

The idea of using the PSP hardware for the determination of model attitude and position was applied to image data from a recent PSP test in 16T (Refs. 6 and 7). The test was performed on a 1:10-scale model of a German Dornier Alpha jet, known as the TST model. Nominal pitch angles in the test were 0, 2, 4, 5, and 6 deg. No intentional yaw or roll angles were introduced. Three  $1024 \times 1024 \times 16$ -bit CCD cameras were used: one mounted above the model, one mounted to the side of the model, and one mounted below the model. Forty-two registration markers were placed on the model. The registration markers consisted of black, circular dots, with diameters of 6.4 mm in model space, or about five image pixels in image space for all three cameras.

Analysis of the data was focused on two tasks: determination of pitch angles from the side-mounted camera, and determination of yaw angles from, separately, the top- and bottom-mounted cameras. Traditional values for pitch, yaw, and roll of the model were also available from digital angle sensors and strain gages on a sting-mounted balance. These angles include corrections for sting deflections under dynamic loading and are believed to be accurate to about 0.02-0.03 deg. All pitch angles quoted here exclude a Mach-number-dependent flow-angle correction that cannot be measured optically. No flow-angle corrections were considered for yaw.

The results demonstrate that the CCD camera system that is used for performing PSP measurements in 16T can be used to measure model pitch and yaw angles with a sensitivity of about 0.003- to 0.005-deg rms. However, absolute accuracies for these measurements appear to be limited to about  $\pm 0.05$  deg, due to apparent motion of the CCD cameras relative to the test article. Some of this camera motion may be the result of the fact that the mounting scheme for the cameras in the TST test was not designed with accurate model P&A determination in mind. However, the results indicate that some of the observed camera motion may be related to large-scale flexing of the test section. Such flexing may not be easy to resolve and would have equal impact on other attitude measurement systems. Independent measurements of camera motion (for example, through the use of gravity-sensing accelerometers) are desirable to resolve remaining ambiguities. Another possible approach to resolving such ambiguities is to perform redundancy checks among P&A measurements from the multiple cameras.

The sensitivities of 0.003- to 0.005-deg rms for pitch and yaw determinations compare favorably with numbers quoted by other researchers. Resolutions in the range "sub-0.01" to 0.05 deg are quoted by other experimenters for the measurement of wing twist by optical means. A direct comparison is difficult, as the results depend on a host of factors, including camera optics, marker size and placement, and data processing.

Further improvements that may be contemplated for the AEDC optical data system include the inclusion of lens distortion effects in the imaging equations, application of the technique to measurement of model deformation, and on-line data processing to provide position and attitude information in real time. Of course, position and angle determinations are not limited to PSP tests.

Rather, they should be applicable in most cases in which it is possible to place registration markers on the surface of the test article.

### 3.5.4 Integration

The use of the PSP image information to provide quantitative data on model deformation and positioning during wind tunnel tests demonstrates the successful accomplishment of project milestone M4, since the PSP system is already integrated into the 16T environment. This methodology can be improved by using video-based systems to increase the data acquisition speed, and this will be looked into during the next FY.

Registration marks placed on the model can be imaged, as shown in Fig. 58, and through the multiple views afforded by the PSP cameras, the position of the model in the flow can be determined.

Such position and attitude determinations were performed recently in 16T on a test of a 1:10-scale model of a German Domier Alpha jet. It was shown that the existing camera system is capable of resolving pitch and yaw angles to within 0.005 deg rms. Sample data are given in Fig. 59. The sensitivities of 0.003- to 0.005-deg rms for pitch and yaw determinations compare favorably with numbers quoted by other researchers.

The cameras of the PSP system are too slow (several seconds to download an image per camera) to couple the measurements to the tunnel control system. Video-based systems that can potentially provide the data rate necessary for AEDC's needs are being investigated.

Analysis of systematic differences between the camera and sting-mounted balance data (as large as  $\pm 0.05$  deg) indicated possible flexing of the wind tunnel walls.

## 3.6 SHEAR STRESS MEASUREMENTS

### 3.6.1 Requirements

Skin friction measurements can provide a better understanding of the behavior of the flow over aerodynamic surfaces, and can therefore be used for development and evaluation of theoretical fluid dynamics models. They can also identify the contribution of viscous drag to the overall aerodynamic losses generated by a test configuration. Accurate measurements over the full surface of a test airfoil can improve the modeling capabilities of the AEDC test environment and reduce the time required to perform aerodynamic testing. Visualization of the state of the boundary layer and the accurate measurement of the shear stress distribution over the entire model surface are important in understanding the cause and effect of configuration changes on the aerodynamic performance of vehicles that are tested in wind tunnels. Shear stress measurements in conjunction with PSP measurements will provide a more complete picture of load distribution on an aerodynamic surface. This information is vital for reducing the development cycle time of flight systems, and it is important for validation of CFD calculations.

A nonintrusive, global technique is desired for measuring the distribution of skin friction magnitude to  $\pm 10$  to 15 percent of the local value, and direction to within  $\pm 1$  to 3 deg on a model surface in a production wind tunnel.

### 3.6.2 Approach

Skin friction measurement techniques can generally be classed as either direct or indirect methods (Ref. 8). With the indirect skin friction measurement techniques (e.g., hot film gages and Preston tubes), a related parameter (e.g., the surface heat flux or impact pressure near the surface) is measured and the skin friction is derived according to the assumptions made in the analysis. Direct techniques (e.g., floating elements and oil films) avoid these assumptions and are therefore preferred, particularly for skin friction measurements in complex flows where the state of the boundary layer is not known in advance.

Shear-sensitive, cholesteric (fatty acid) liquid crystals have been used to visualize boundary-layer transition and flow separation on wings in production wind tunnels at AEDC, as discussed in Section 3.1.2. The rapid response and reversible nature of the liquid crystal material makes it possible to acquire boundary-layer information as fast as test conditions can be changed for as long as sufficient material remains on the model surface. The helical-shaped molecules in the liquid crystal material selectively scatter white light so that different wavelengths are scattered in specific directions. The particular color that is observed at a stationary viewing location is a function of illumination angle and local shear stress, as well as other environmental factors.

More recently, researchers at NASA Ames (Refs. 9 and 10) have been developing a system to measure the distribution of surface shear stress vectors using a liquid crystal coating. They report that for a nearly perpendicular lighting of a flat surface and a constant viewing angle above the surface, the observed hue is a function of surface shear stress and that the maximum value of hue occurs when the flow vector is aligned with the viewing direction. By recording images at a number of viewing angles, researchers can determine the magnitude and direction of the shear stress vector.

The objective is to transition this technology to a production wind tunnel. The challenge in transitioning this technology comes from differences in the physical environment between the laboratory and a production facility. The laboratory results were obtained on a flat surface at constant viewing angles with virtually unlimited optical access to the model. In a production environment, there is limited optical access of an arbitrarily shaped model that can move with six degrees of freedom. The approach selected to address this challenge was to define the light-scattering characteristics of the liquid crystal material as functions of lighting angle, viewing angle, and applied shear stress. The variation in lighting and viewing angle would simulate differences in model shape and/or movement. The repeatability of the measurement of the light-scattering characteristics as functions of these variables is a key issue in determining the feasibility of transitioning the technology to the production environment.

Another technique being pursued provides the capability of making a point measurement with an optically scanned micro-mechanical device (Metro-Laser SBIR). This concept is being pursued, but is not yet ready for examination of its applicability to 16T. Initial investigation indicates that this technique would be very difficult to implement.

### 3.6.3 Capability Description

The NASA technique, which measures global shear stress by using the shear-sensitive liquid crystals, was set up in a laboratory using hardware borrowed from NASA. A Sony XC-003 color CCD camera and MATROX Corona 8E frame grabber were procured and added to the system to acquire the data. A picture of the hardware configuration is shown in Fig. 60. An investigation was begun into the applicability of the technique for wind tunnel testing in 16T. A flow device borrowed from NASA was used to provide the flow conditions needed for calibrating the shear stress response of the liquid crystals. This device has proved to be somewhat difficult in achieving steady flow conditions for certain operational parameters; this is apparently related to choking of the flow that occurs in the air supply line. A skin friction balance which utilizes small, sensitive strain-gage balances is needed to aid in the calibration of this device.

Preliminary calculations were performed to estimate the range of shear stress expected for 16T. It was determined that shear forces between 0.005 and 4 psf were possible for Mach numbers between 0.2 and 1.0. This work needs to be continued to determine whether the range of conditions that can be attained in a flow device is applicable to the 16T performance envelope.

In a typical experiment, an airbrush was used to spray a mixture of one part liquid crystals to nine parts solvent onto the lower wall of the flow device, and the device was then viewed through a window on the upper wall. Images were recorded to evaluate the change in color observed as a function of viewing angle and magnitude of shear stress. The surface coated with the liquid crystals was illuminated by a white light source directed normal to the surface. The color camera was positioned at an angle of approximately 30 deg above the surface. Images were obtained at 30-deg intervals circumferentially about the center of the viewing window from 0 (looking downstream) through 180 (looking upstream) to approximately 330 deg. This procedure was repeated for at least three values of shear stress. Also, calibration at 0 deg was repeated several times to establish data repeatability.

The first acquired images appeared to have too much liquid crystal material applied to the surface. This conclusion was reached because the material did not appear to remain stationary in the video, but appeared to be flowing along the surface. Also, the application technique resulted in a grainy image that was caused by drops or splattering of the material. The challenge with applying the material in a uniform and adequately thick layer is that the material is transparent until a shearing stress is applied. In order to visualize the material during application, a small brush was used to stress the material; however, this was unsatisfactory because the brush strokes remained visible in the images. Several spraying techniques were tried with varying degrees of

success. The most promising approach appears to be to determine the optimum amount of liquid crystals per unit area to be covered, place the required amount of material in an airbrush for the area to be covered, and continue spraying over the area until all the material in the airbrush has been used (taking care to cover the surface as evenly as possible).

Laboratory data have been acquired for two formulations of liquid crystals in an attempt to replicate the results reported by NASA. NASA has reported that the hue response of the liquid crystals produces a Gaussian distribution with viewing angle with the maximum centered along the direction of flow, and a minimum beginning at  $\pm 90$  deg. In the AEDC measurements, a maximum was observed at the same location as seen at NASA, but an additional maximum was observed in a direction counter to the flow (which was not reported by NASA) as well as an anomaly at  $\pm 45$  deg. A series of experiments was initiated to validate these results. The anomaly at  $\pm 45$  deg was apparently caused by a combination of a nonuniform surface coating and a problem with defining the area to be sampled as a function of viewing angle. This anomaly was eliminated in later experiments; however, the second maximum in hue at around 180 (or  $-180$ ) deg is still present. Further experiments are in progress to determine the cause of this second, unexpected maximum. The outcome of these experiments will be important in determining the feasibility of applying the liquid crystal technique in a production facility. If these observations are correct, it may not be possible to uniquely determine flow direction or skin friction magnitude. An example of the shear stress image data is shown in Fig. 61. The hue of the images changes from green (0 deg) to yellow (60 deg) to yellow-brown (120 deg) to brown (180 deg). A plot of hue versus observation angle is shown in Fig. 62.

### 3.6.4 Integration

The shear stress and skin friction diagnostic system will not be integrated during the course of this project because the technique is not sufficiently mature at this time.

## 3.7 MULTIPLE DIAGNOSTICS INTEGRATION TEST

For the DGV and BLT integration test, the systems were set up in Building 607. A seeded Mach 2.7 jet was installed to simulate the 16T flow, as described in Section 3.2. The ODC and BLT computers were set up on a table as shown in Fig. 63, with the ODC on the right. The DGV and BLT integration project milestone (M8) was accomplished May 19, 2000. The ODC was used to control the DGV diagnostic system remotely. In the same configuration, the ODC also directed the BLT diagnostic system to acquire data from the BLT camera, as described in Section 3.1.

This demonstration could not use the actual 16T server due to operational and security issues. The demonstration was accomplished with the aid of a simulator. A Unix computer (named ivan) was installed in the ELA building (Building 1077) and connected to the OIS. A replica of the 16T database was accessed and pertinent run parameters transferred back and forth. Each data packet was sent and received five times, employing the protocol used by the PSP system. The control

window for the 16T interface is shown in Fig. 64 for the systems upgraded by the 16T Sustainment Program. A similar window for the nonsustainment systems is shown in Fig. 65.

### 3.8 16T WIND TUNNEL TEST

The programming to modify the LVS software for the local system and the ODC was completed for a JDAMS test in the 16T wind tunnel test. This was necessary because this test was not using the sustainment data system on the CTS cart. The 16T software was reconfigured to read only the ADS tunnel conditions file from the 16T network. The ODC, LVS, and BLT computer systems were installed for the 16T test. The BLT and LVS PCs were placed under the control of the ODC. The ODC was connected to the 16T network via ethernet to read the ADS tunnel data file.

The BLT camera installation is shown in Fig. 66. The BLT PC placement is shown in Fig. 67. The LVS system was installed in 16T; the laser is shown in Fig. 68. The laser scan controller is shown in Fig. 69. The galvanometer placement is shown in Fig. 70. The LVS PC was installed in a room off of the 16T control room as shown in Fig. 71. The ODC was placed in the same room as shown in Fig. 72.

During actual test runs, the ODC obtained tunnel data and acquired images from the BLT system. These are shown in Fig. 73 and Fig. 74. These test data were acquired on July 28 and 31, 2000. Three tests using the ODC occurred on July 28, July 31, and August 1, 2000. The ODC acquired 100 frame infrared image sequences of the test model while the tunnel was on condition. The image sequences and the IRIG times were sent back to the ODC for immediate viewing. The tunnel conditions were acquired and saved to file for viewing later. These three tests were not dedicated BLT test runs.

The last test in 16T using the ODC occurred on August 24, 2000. This was a dedicated test for the BLT and LVS. The BLT was the first to acquire data. The model was pitched to 26 deg for optimal viewing by the infrared camera. The ODC then acquired four 100-frame image sequences per model position. The image sequences were sent back to the ODC for immediate viewing. The model was either rolled or pitched down, then back up, with a new tunnel condition when the ODC acquired four more 100-frame image sequences. During this time the ODC acquired the tunnel conditions from the 16T ADS computer and saved them to file. The BLT portion of the test ended up with 630 MB of infrared 100-frame image sequences and IRIG times with the tunnel conditions.

The LVS was next to acquire data. Before the test started for the LVS, a frame was drawn with four lines to be used by the ODC during the LVS test. The ODC initialized the laser show and displayed the four lines on the test model. The lines were then moved up and down the model. Next, the lines were stretched to widen the space between the lines to see the visual flow better. No data were acquired by the ODC from the LVS system. The data were acquired by

recording the video during the test. Tunnel conditions were acquired by the ODC during the test and saved to file.

The ODC was successfully used to control the BLT and LVS systems and to acquire data from these systems during a live 16T wind tunnel test. The ODC also successfully acquired the tunnel conditions from the 16T ADS computer during a live 16T wind tunnel test.

## **4.0 CONCLUSIONS**

### **4.1 SUMMARY OF WORK**

The purpose of the ODS project was to develop an integrated optical diagnostics system for AEDC's 16-ft Transonic Wind Tunnel (16T) testing area. This facility provides aerospace system developers and testers the tools needed to reduce the total time required to conduct a wind tunnel test program. It enables testers to 1) greatly reduce the time and cost required to design and manufacture wind tunnel models; 2) reduce model assembly time at the test facility; 3) essentially eliminate model instrumentation setup time; 4) significantly reduce tunnel setup time; and 5) offer customers the potential to combine multiple wind tunnel tests into a single entry and test run.

All project milestones except the integration of a shear stress/skin friction technique have been met. This milestone was not achieved because the shear stress diagnostic technique lacked sufficient maturity to enable integration. A chart of the milestones and demonstrations scheduled in the program is shown in Table 1.

The milestones that were met demonstrate the development, evaluation, and staging of optical instruments for integration into the 16T test environment. A capability for annotating the image data acquired by the PSP system has been developed whereby test configuration details can be documented. The PSP system has also been used to determine model attitude and position information. The ODC has been implemented and interfaced to the BLT, DGV, and LVS diagnostic systems. Operational control of these diagnostics through a fiber-optic reflective memory network has been achieved in the lab and test environment. Simultaneous control of multiple diagnostics has also been achieved.

### **4.2 RECOMMENDATIONS**

The development of nonintrusive optical diagnostic techniques and the pursuit of their integration into the 16T wind tunnel environment must be continued to strengthen AEDC's ability to aid aerospace system developers and testers in their constant efforts to produce their products faster and cheaper. As current diagnostic technologies become more sophisticated and new concepts are developed, the 'plug and play' method of incorporating them into the test facility should be a continual part of the facility modernization methodology. As an example, it is expected that advancements from pressure, temperature, and shear-sensitive paint research will occur in the near future; these should be included in this integration concept when they become



mature. An avenue of funding needs to be pursued to accomplish this adaptation of new results and new technologies. This will help ensure that AEDC remains a premier ground test facility for advanced aerospace weapon system development. AEDC should also continue to work closely with NASA test centers and industry to develop a coordinated national program for wind tunnel test technologies.

The ultimate vision to develop the capability to immediately display locally all final/reduced optically measured test data from any perspective graphically at the console should still be a goal for the future. This will involve the development of extremely high-speed computing, processing, and display capabilities as well as software to allow enhanced comprehensive comparisons of theoretical time-critical results, computational (CFD, etc.) results, and experimental optical-diagnostic measurements in a manner suitable for test support. To reach this ultimate vision, follow-on funding will have to be found.

### REFERENCES

1. Sinclair, D. W. "Measurement Techniques Applied in a Production Wind Tunnel Facility at Transonic Speeds." AIAA-96-2181, 19th AIAA Advanced Measurement and Ground Testing Conference, New Orleans, LA, June 1996.
2. Smith, S. "The Use of Liquid Crystals for Surface Flow Visualization." AIAA-90-1382, AIAA 16th Aerodynamic Ground Testing Conference, Seattle, Washington, June 18-20, 1990.
3. Schneiderman, A. M. and Sutton, G. W. "Laser Planogram Measurements of Turbulent Mixing Statistics in the Near Wake of a Supersonic Cone." *Physics Fluids*, 1970, Vol. 13, pp. 1679-83.
4. Diemunch, G. and Prenel, J. P. "A Compact Light Sheet Generator for Flow Visualizations." *Opt. Laser Technol.*, Vol. 19-3, 1987, pp. 141-144.
5. Sellers, M. E. and Brill, J. A. "Demonstration Test of Pressure Sensitive Paint in the AEDC 16-ft Transonic Wind Tunnel Using the TST Model." AIAA 94-2481, 18th AIAA Aerospace Ground Testing Conference, Colorado Springs, CO, June 1994.
6. Ruyten, W. M. "Toward an Integrated Optical Data System for Wind Tunnel Testing." AIAA-99-0181, 37th AIAA Aerospace Sciences Meeting and Exhibit, Reno, NV, January 1999.
7. Ruyten, W. M. "Model Attitude Measurement with an Eight-Camera Pressure Sensitive Paint System." AIAA-2000-0831, 38th AIAA Aerospace Sciences Meeting and Exhibit, Reno, January 2000, NV.
8. Buttsworth, D. R., Elston, S. J., and Jones, T. V. "Skin Friction Measurements on Reflective Surfaces Using Nematic Liquid Crystal," *Experiments in Fluids*, Vol. 28, 2000, pp. 64-73.



9. Reda, D. C. "Measurement of Surface Shear Stress Vectors Using Liquid Crystal Coatings." *AIAA Journal*, Vol. 32, No. 8, 1994, pp.1576-1582.
10. Reda, D. C. et al. "Areal Measurements of Surface Shear Stress Vector Distributions Using Liquid Crystal Coatings." AIAA 96-0420, 34th AIAA Aerospace Sciences Meeting, Reno, Nevada, January 1996.

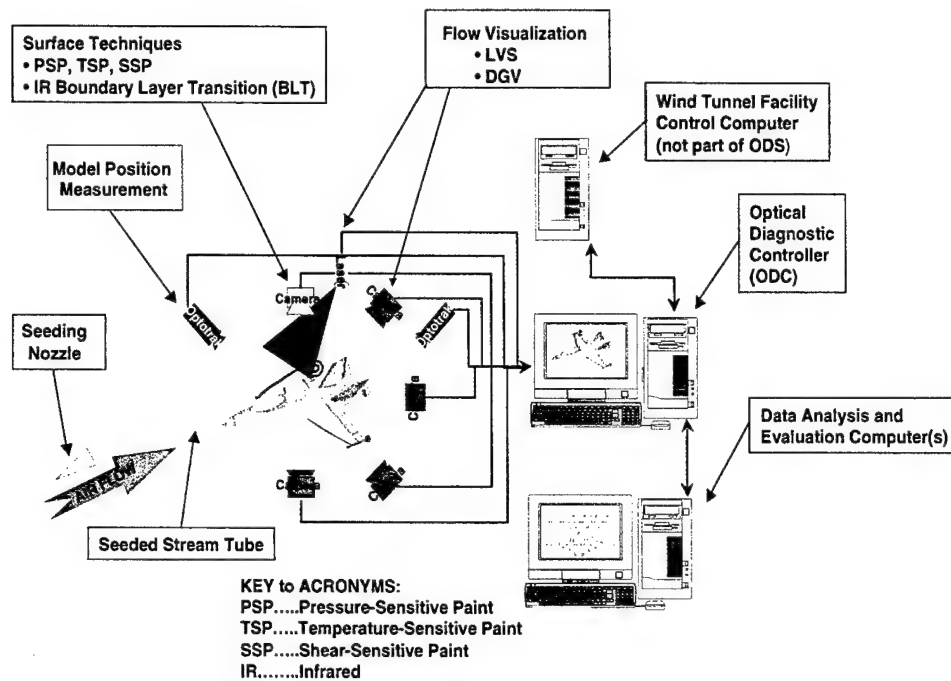


Figure 1. Integrated Optical Diagnostics System

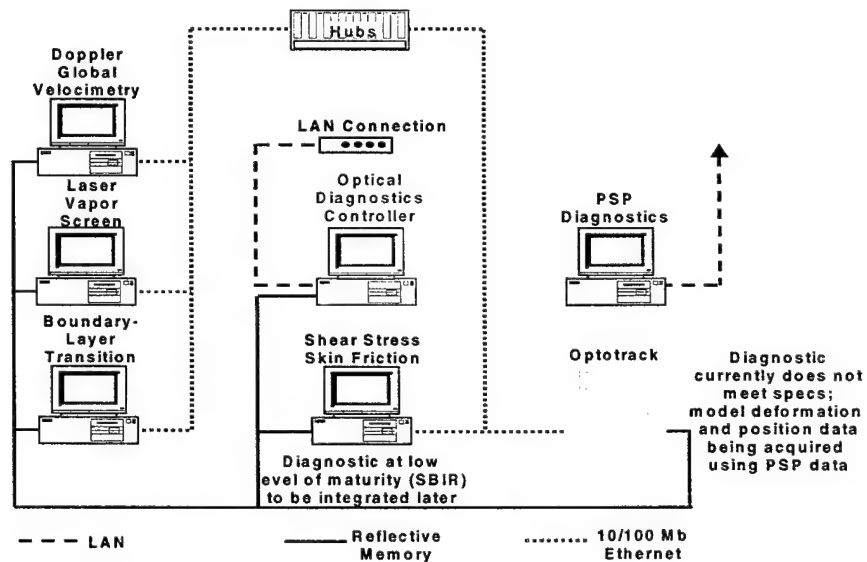
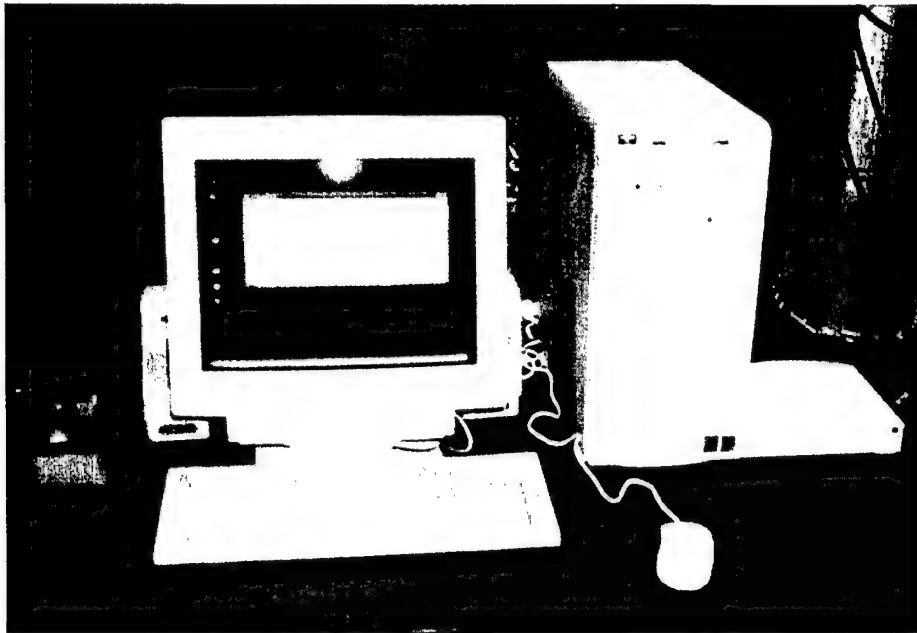
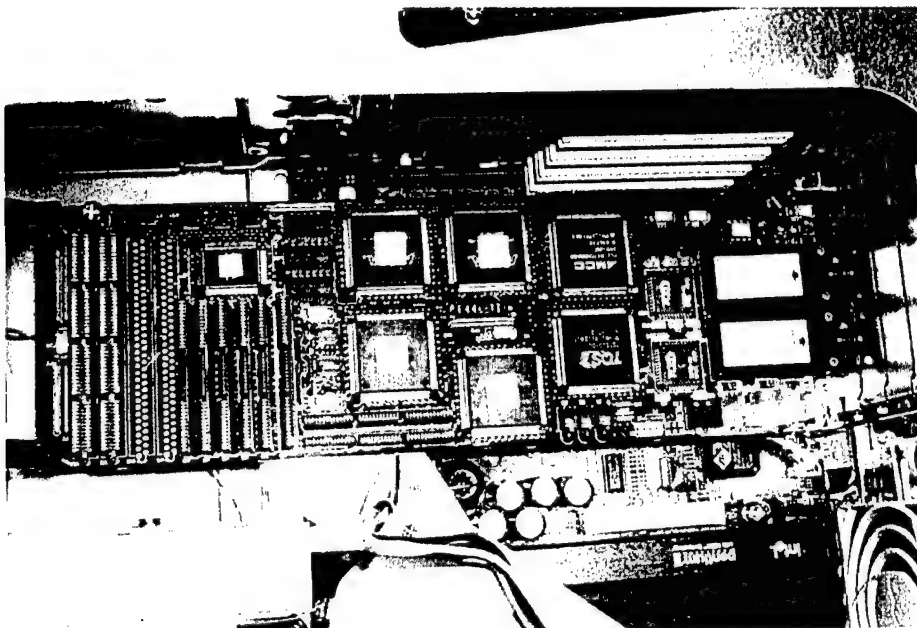


Figure 2. Hardware Configuration of ODC and Optical Diagnostics



**Figure 3. ODC Computer System**



**Figure 4. VMIC Reflective Memory Card**

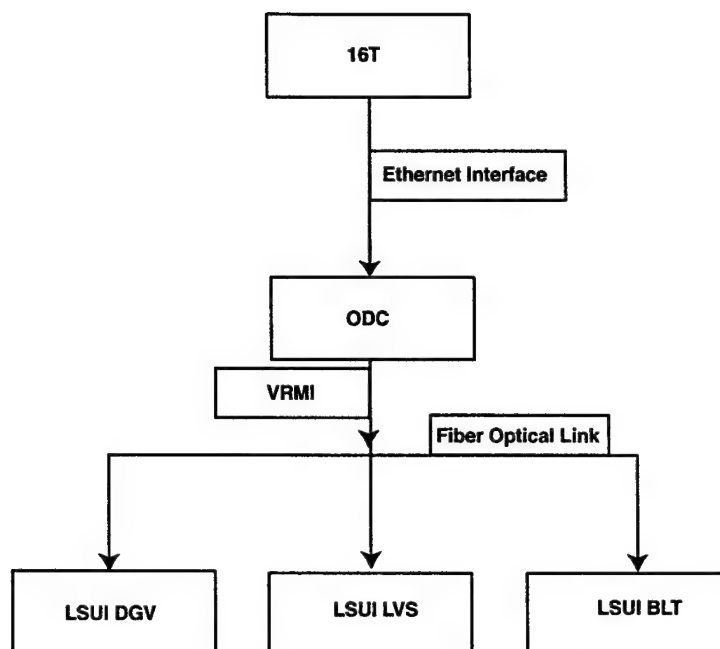


Figure 5. Conceptual Block Diagram of the ODS Software

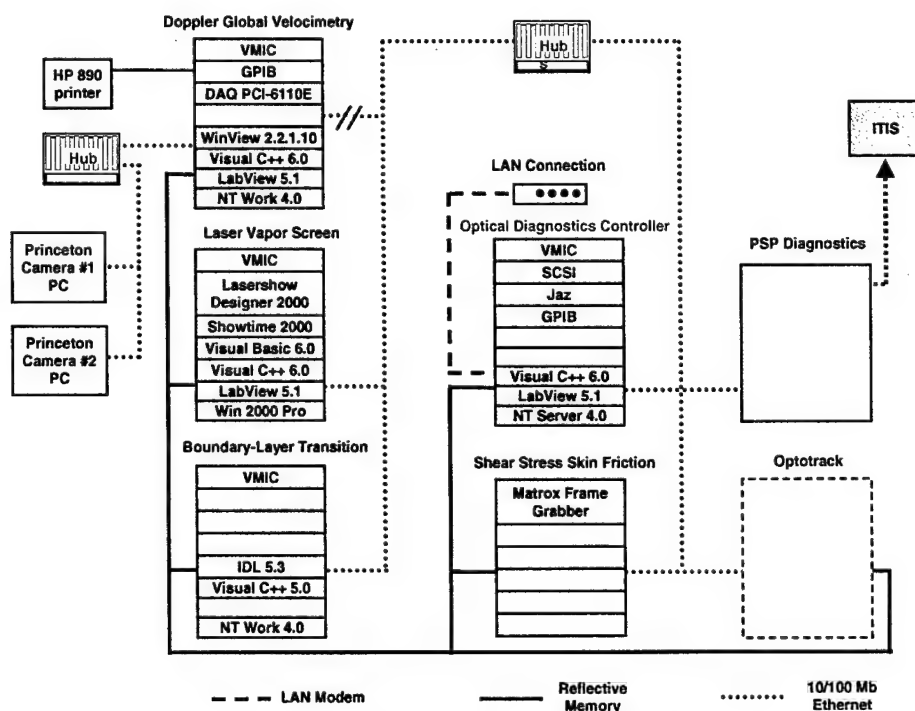


Figure 6. Hardware Population of ODS

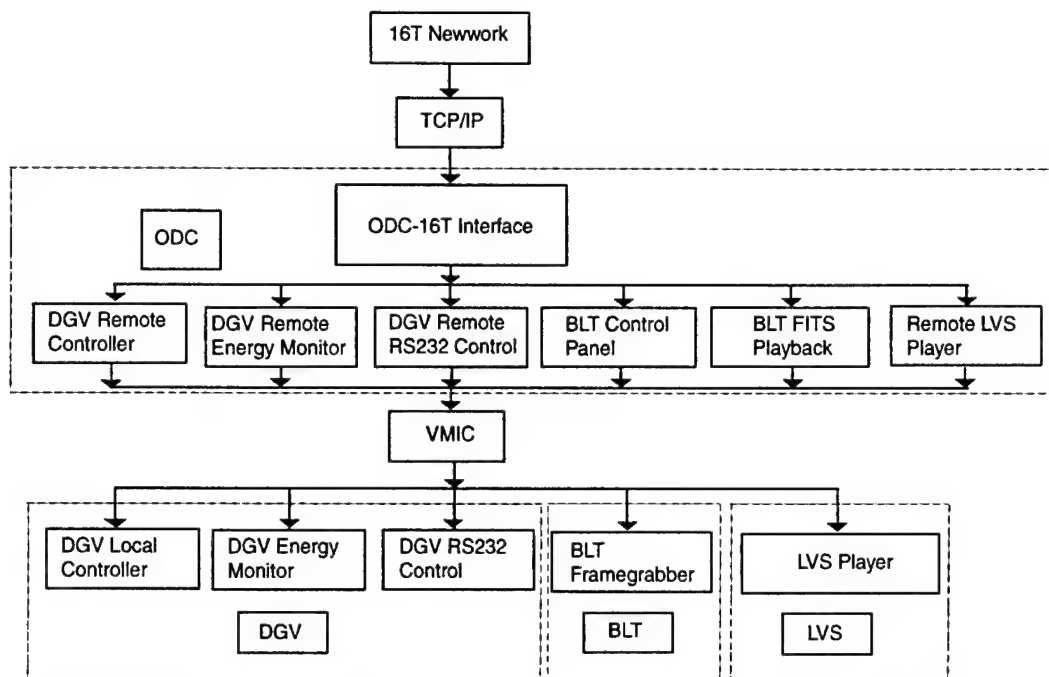


Figure 7. Functional Flow of the ODS Software

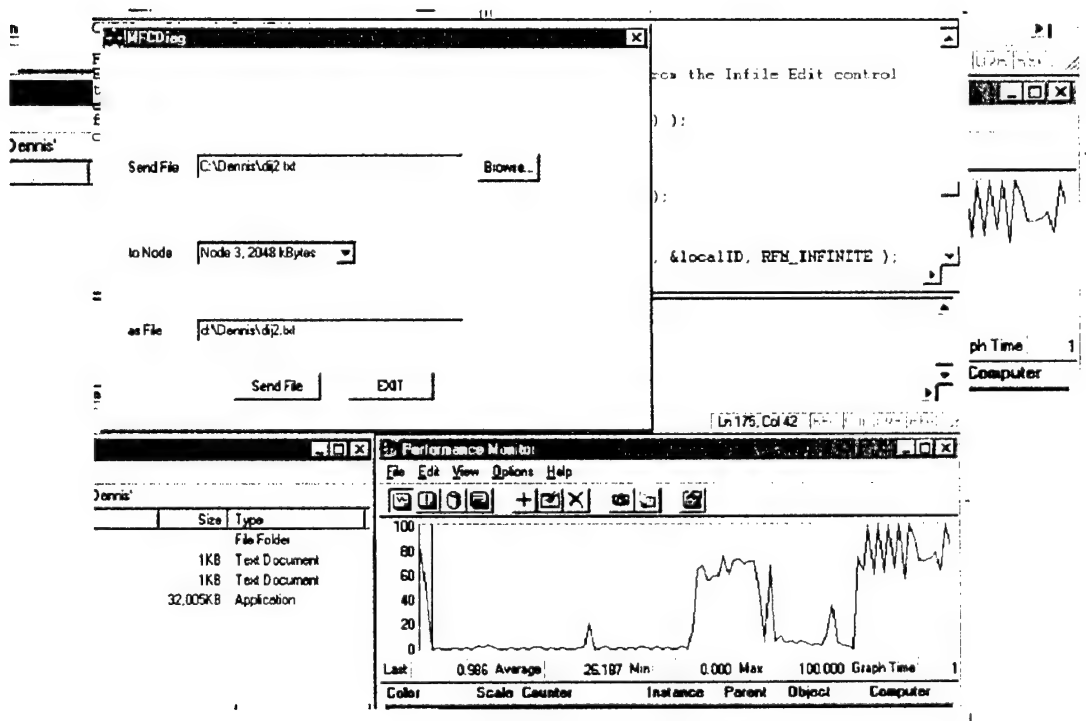


Figure 8. Image of ODC Computer Screen

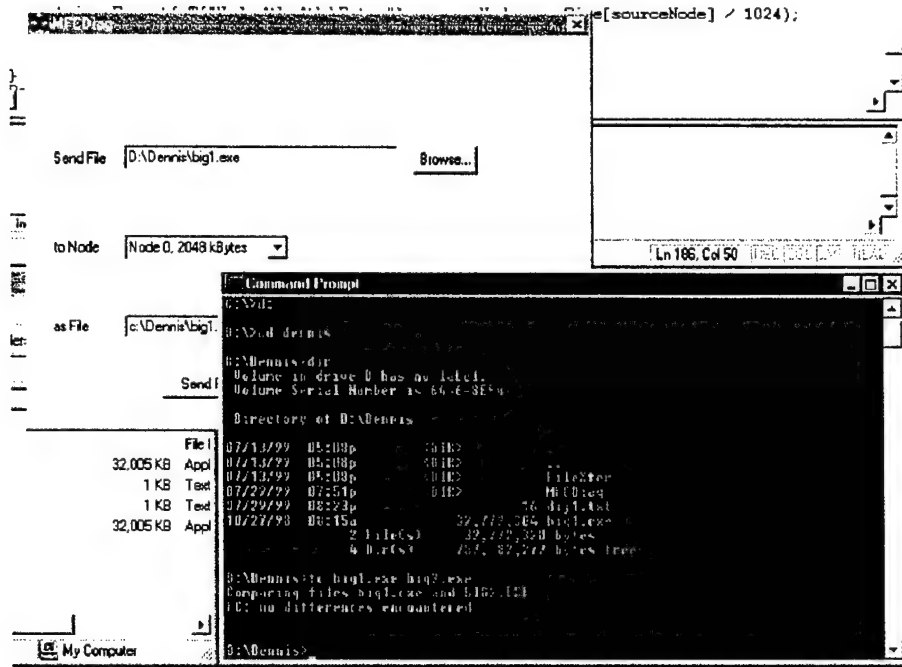


Figure 9. Image of the BLT Computer Screen

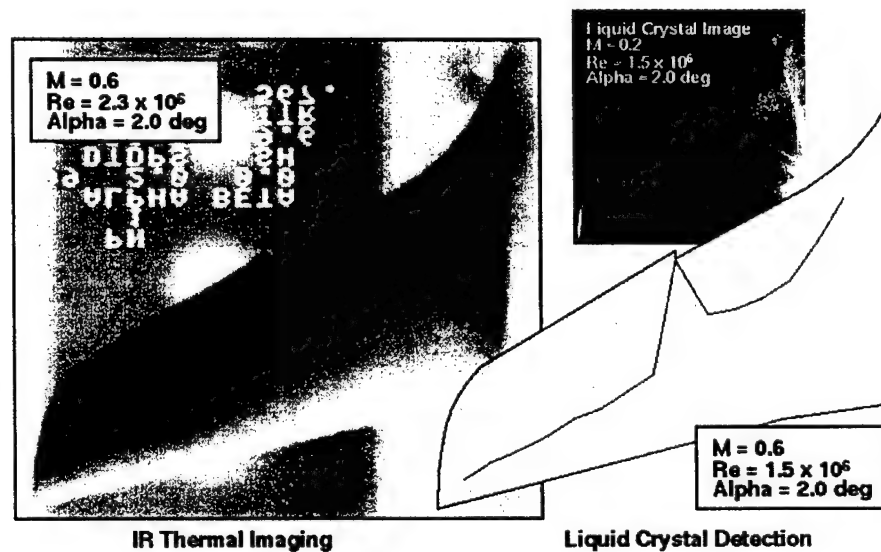


Figure 10. Comparison of IR Thermal Imaging and Liquid Crystal Detection Techniques



Figure 11. BLT Camera

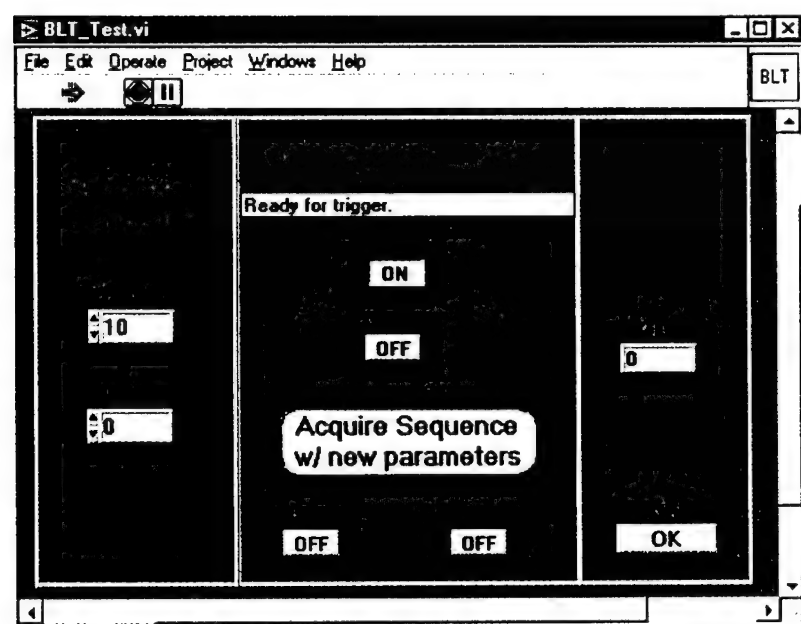


Figure 12. LabView® Program for Control of BLT Camera from ODC

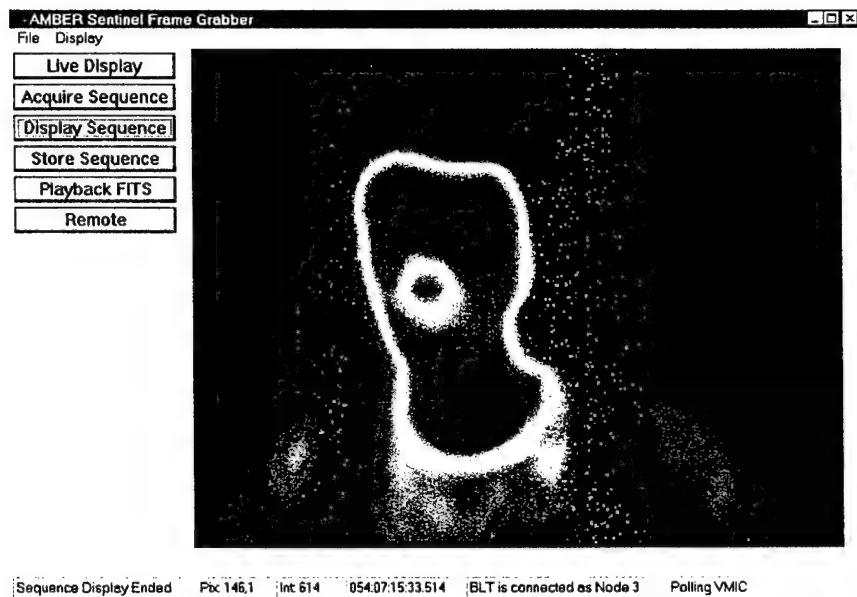


Figure 13. BLT Data Acquired by BLT Camera and PC

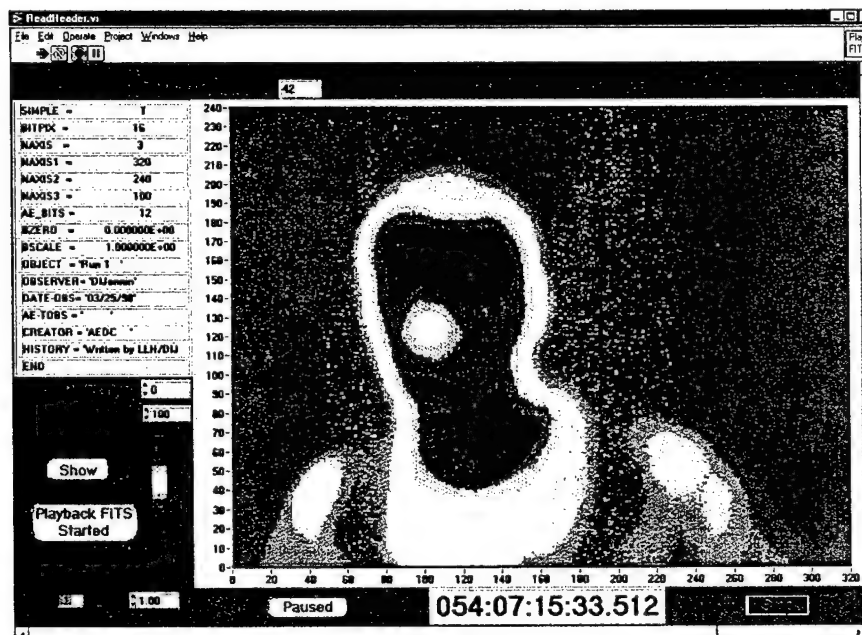


Figure 14. Transferred BLT Data Displayed on ODC PC



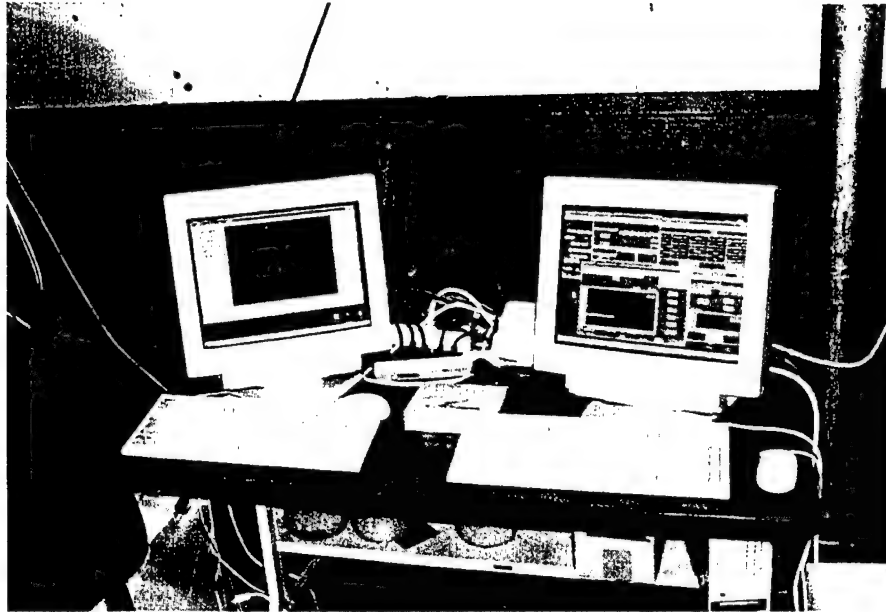


Figure 15. ODC and BLT Computers

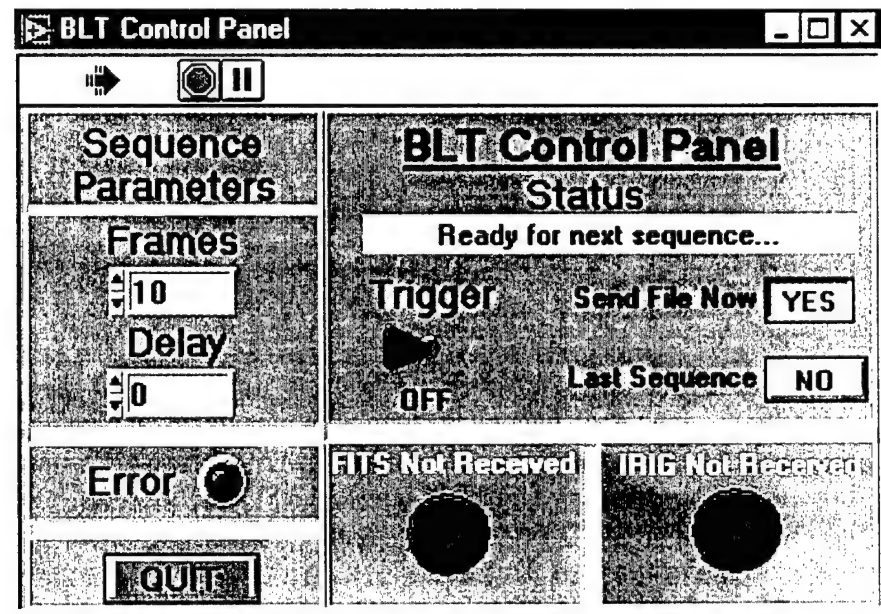


Figure 16. BLT Control Panel on the ODC

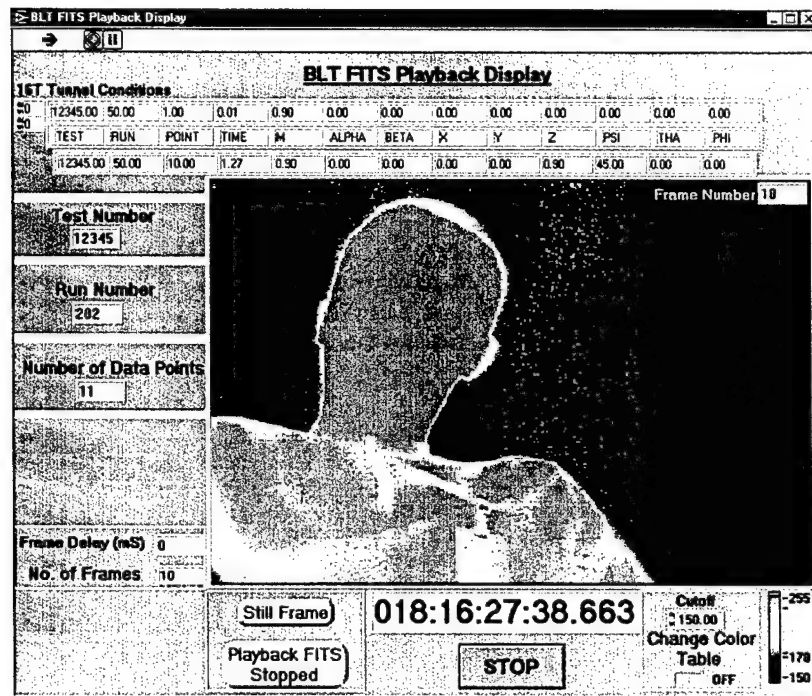


Figure 17. BLT FITS Playback Display

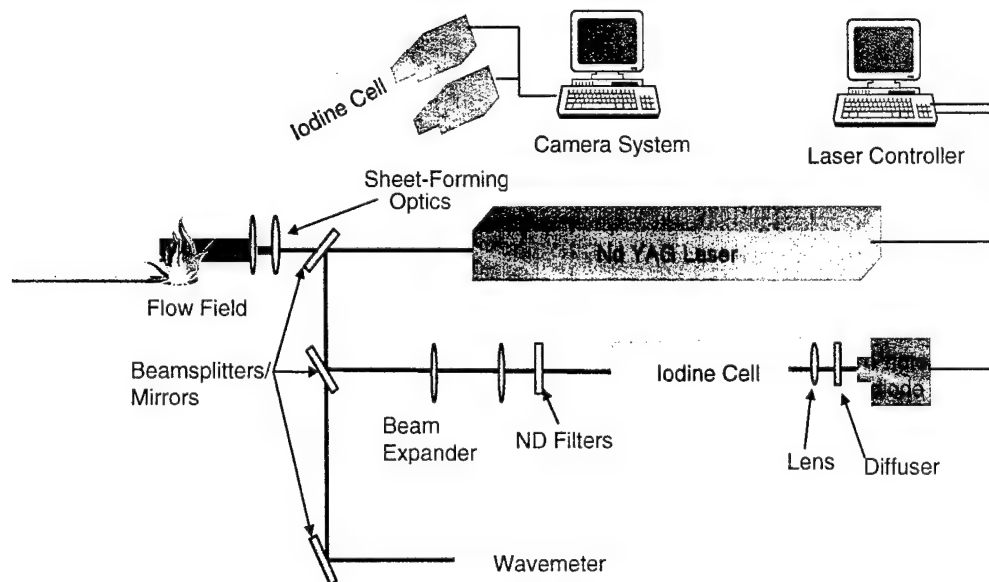


Figure 18. DGV Setup

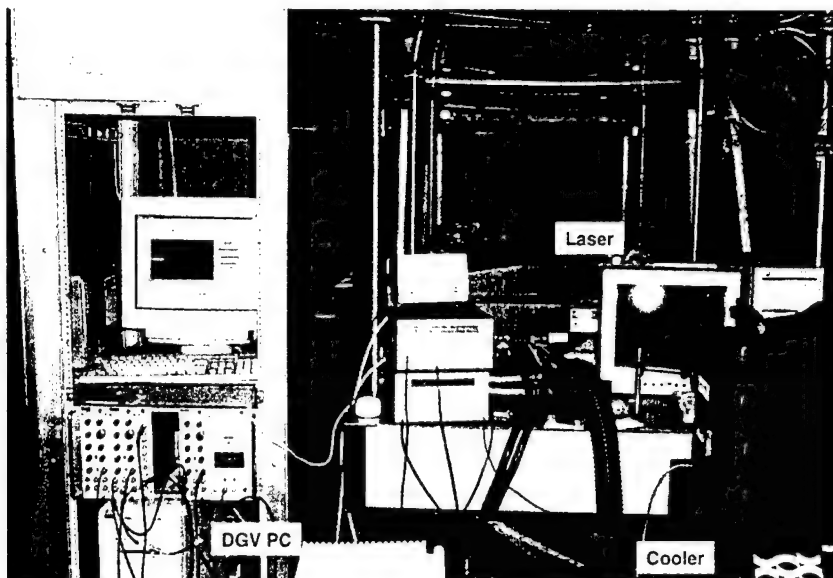


Figure 19. DGV Hardware Configuration

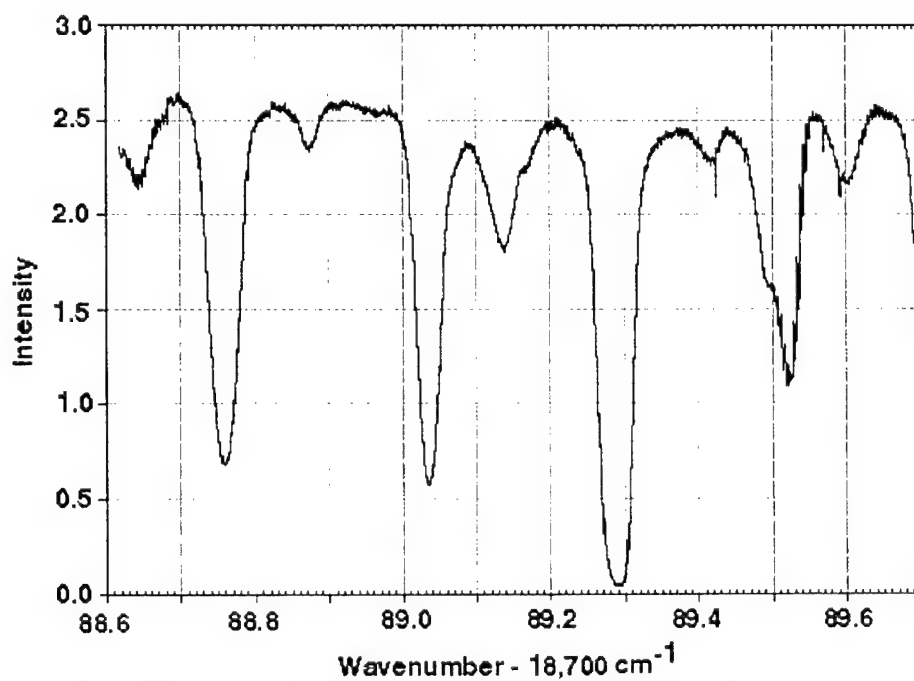
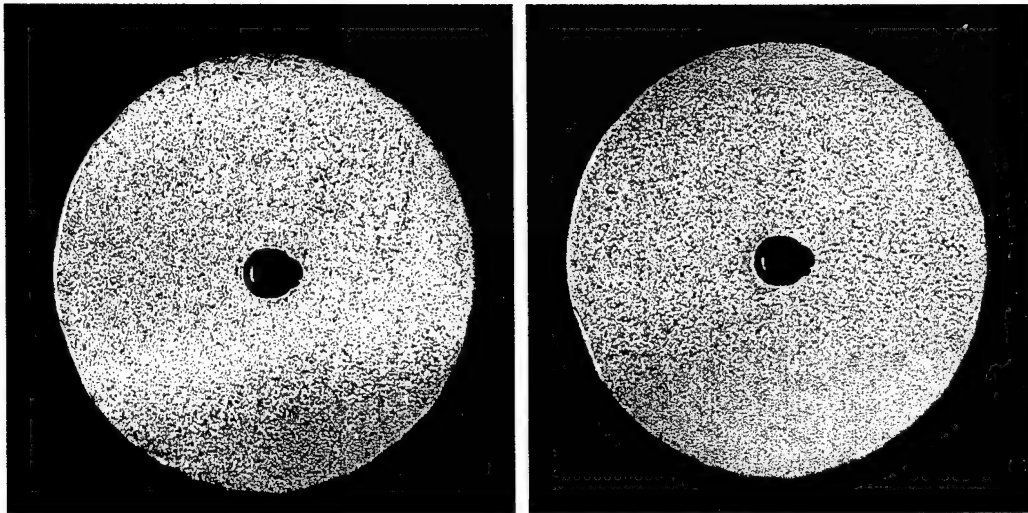
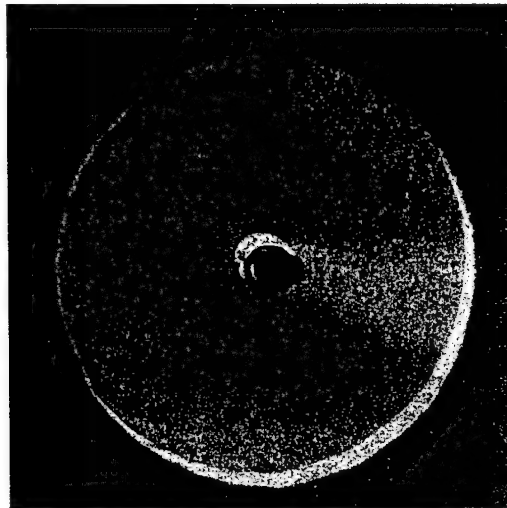


Figure 20. Typical Iodine Absorption Spectrum at 20 torr, 80°C



**a. Filtered Image**

**b. Unfiltered Image**



**c. Intensity Ratio of Filtered to Unfiltered Images**

**Figure 21. Images of Static Wheel**

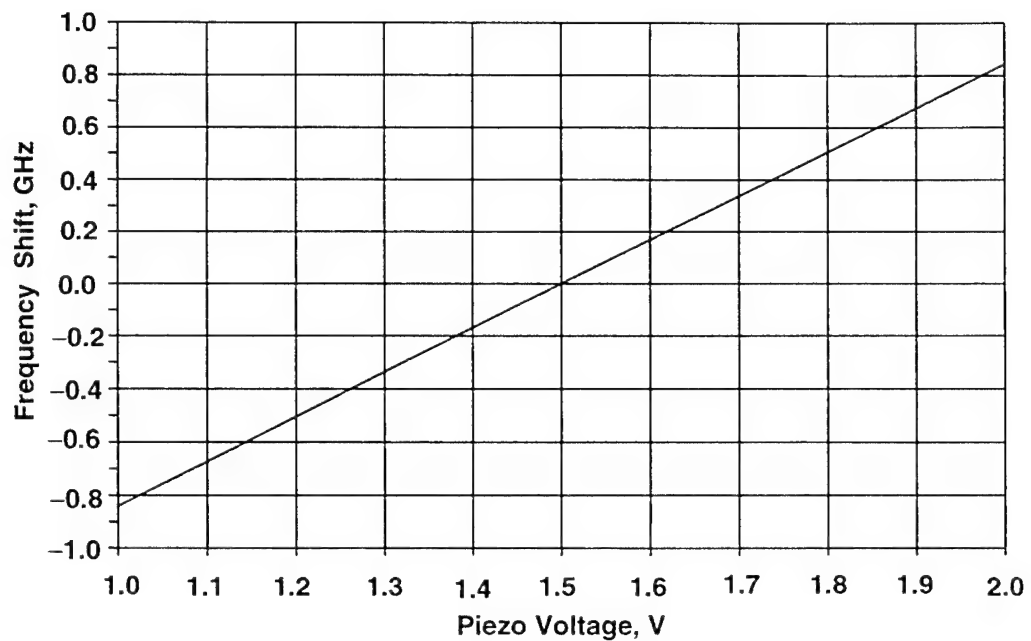


Figure 22. Frequency Shift versus Piezo Voltage

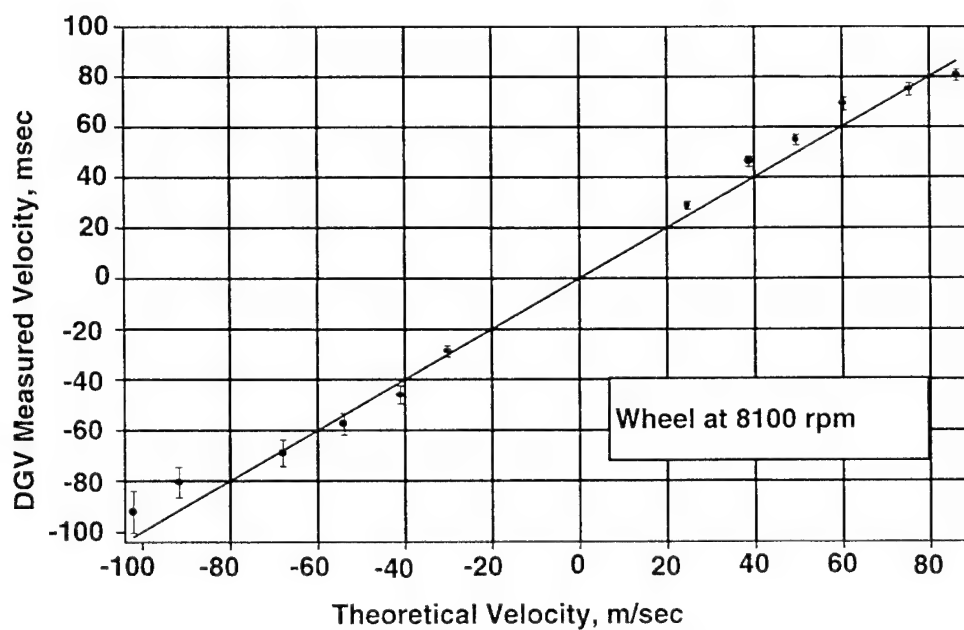
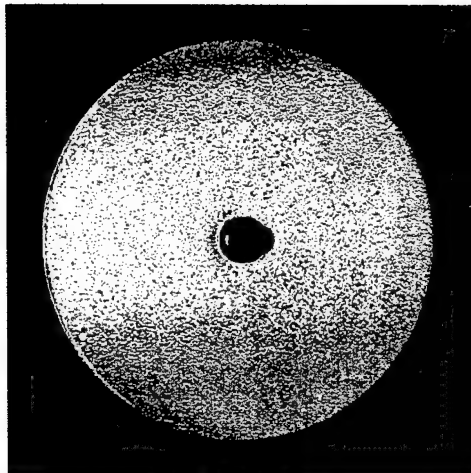
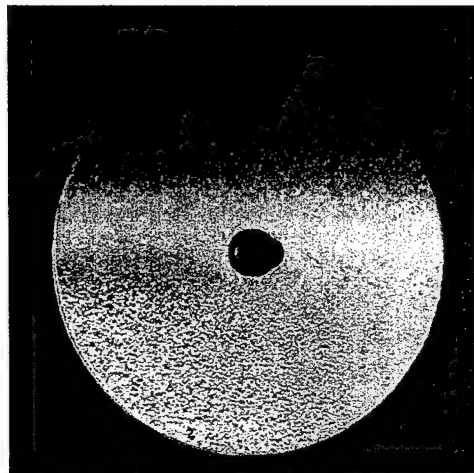


Figure 23. DGV Measured versus Theoretical Velocity



**a. Filtered Image**



**b. Unfiltered Image**



**c. Intensity Ratio of Filtered to Unfiltered Images**

**Figure 24. Images of Rotating Wheel**

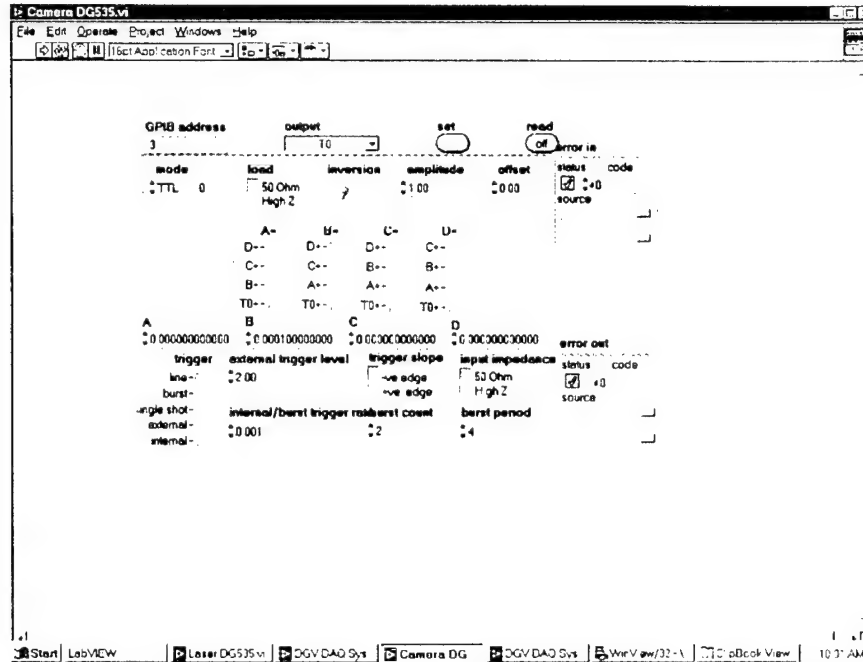


Figure 25. LabVIEW® Program for Control of DGV Camera from ODC or DGV PC

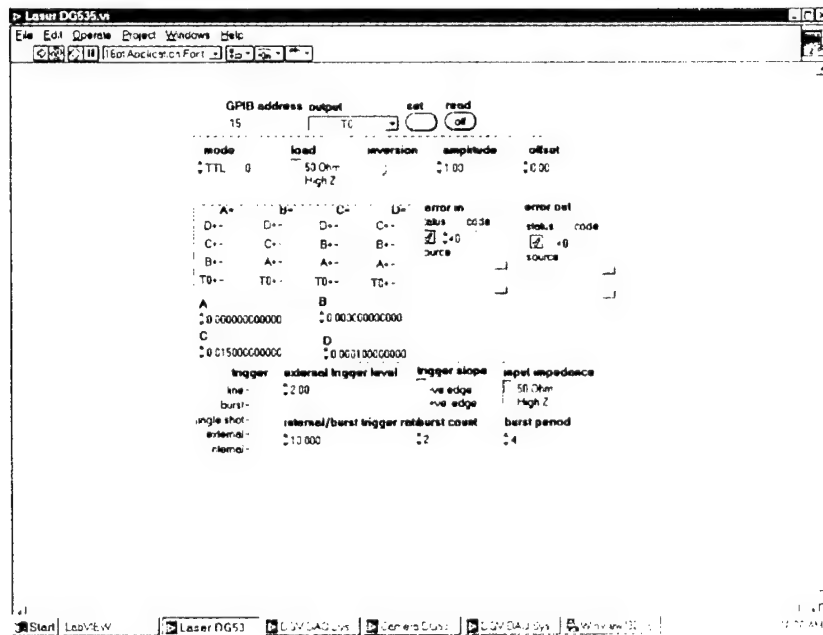


Figure 26. LabVIEW® Program for Control of DGV Laser from ODC or DGV PC

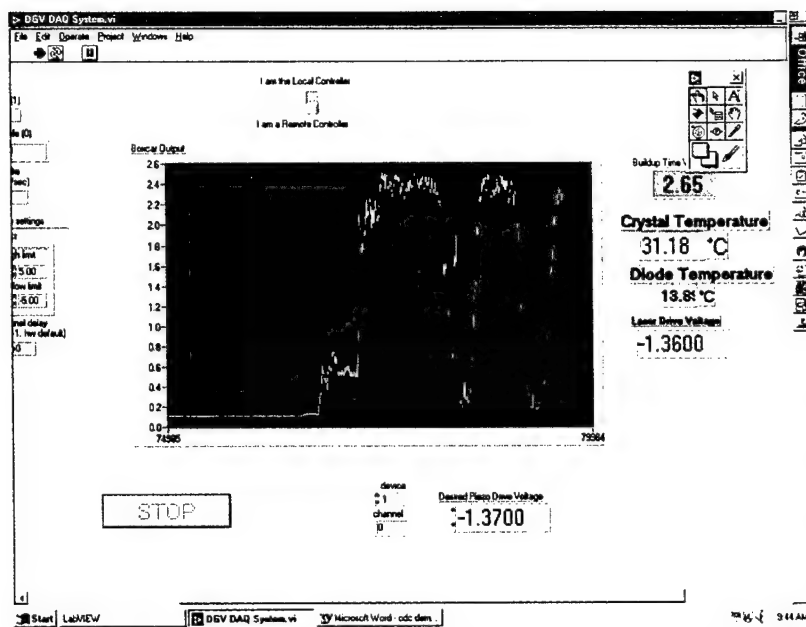


Figure 27. LabView® Program for Control of DGV System from ODC or DGV PC

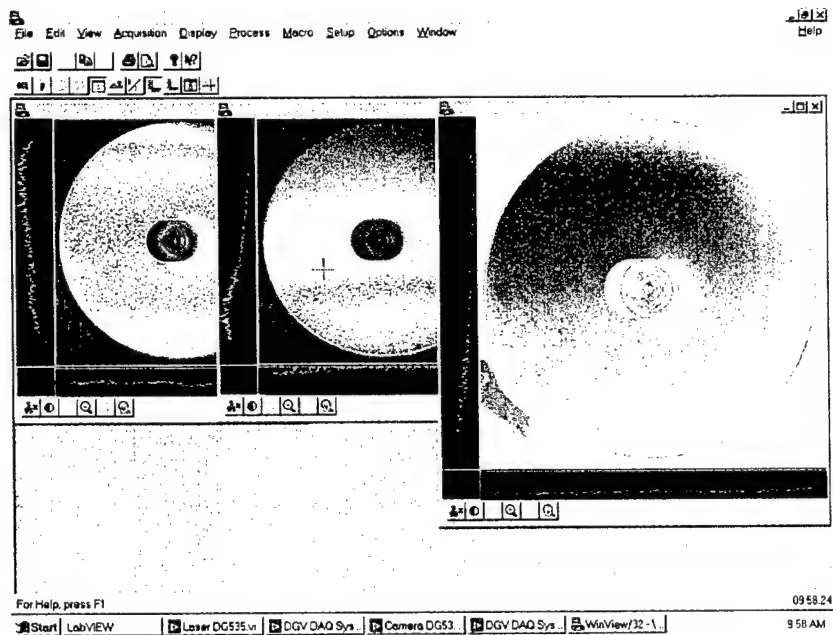


Figure 28. WinView Program Displaying DGV Camera Data and Processing



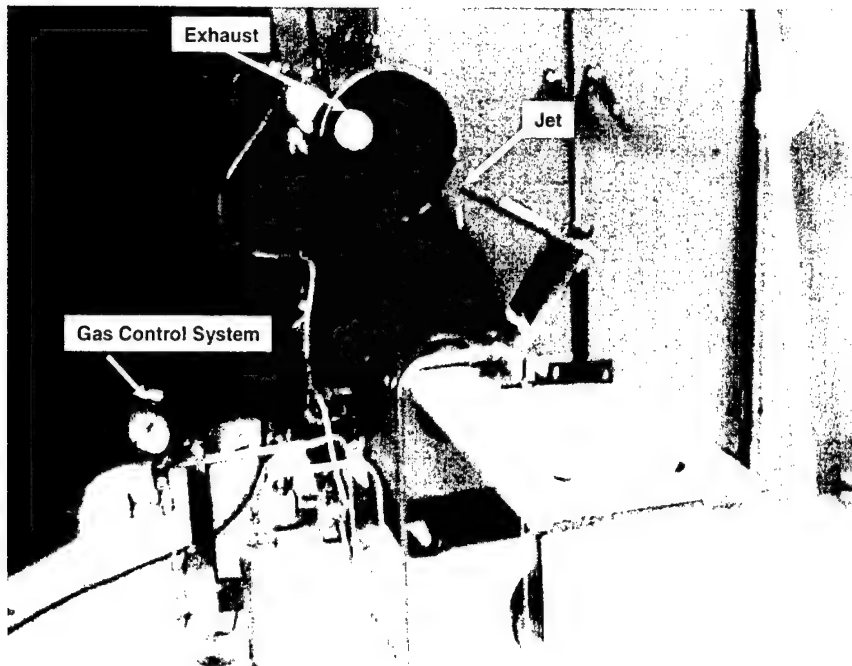


Figure 29. DGV Test Jet with Exhaust Diffuser

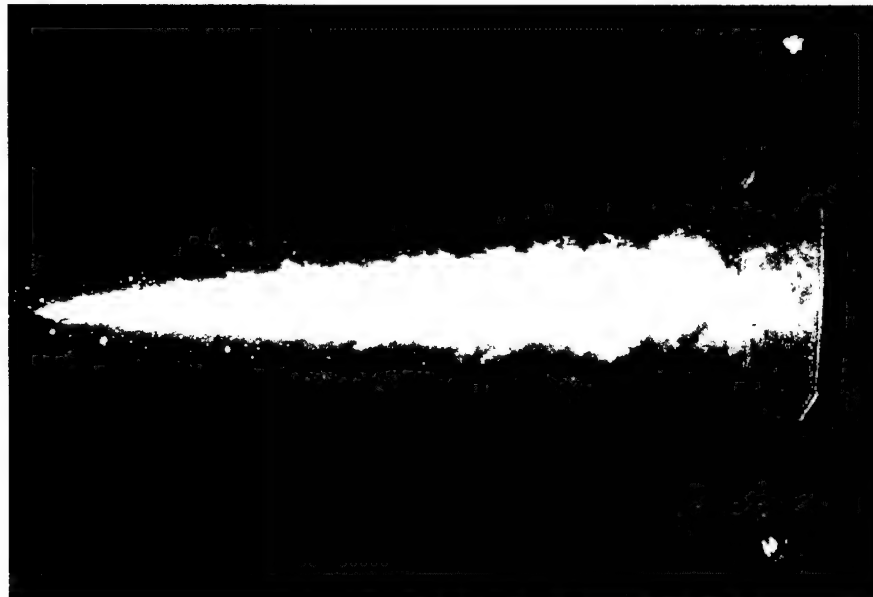
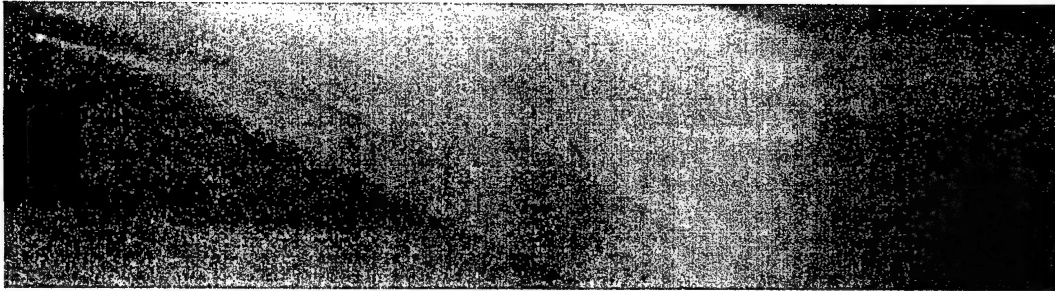
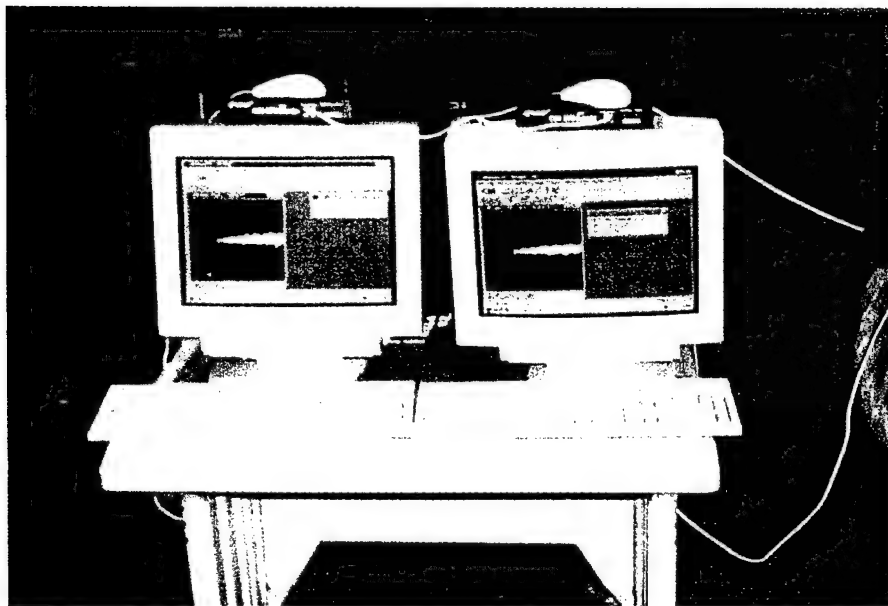


Figure 30. Image of Jet Flow



**Figure 31. Shadowgraph Image of Jet Flow**



**Figure 32. DGV Monitors and Control Keyboards**

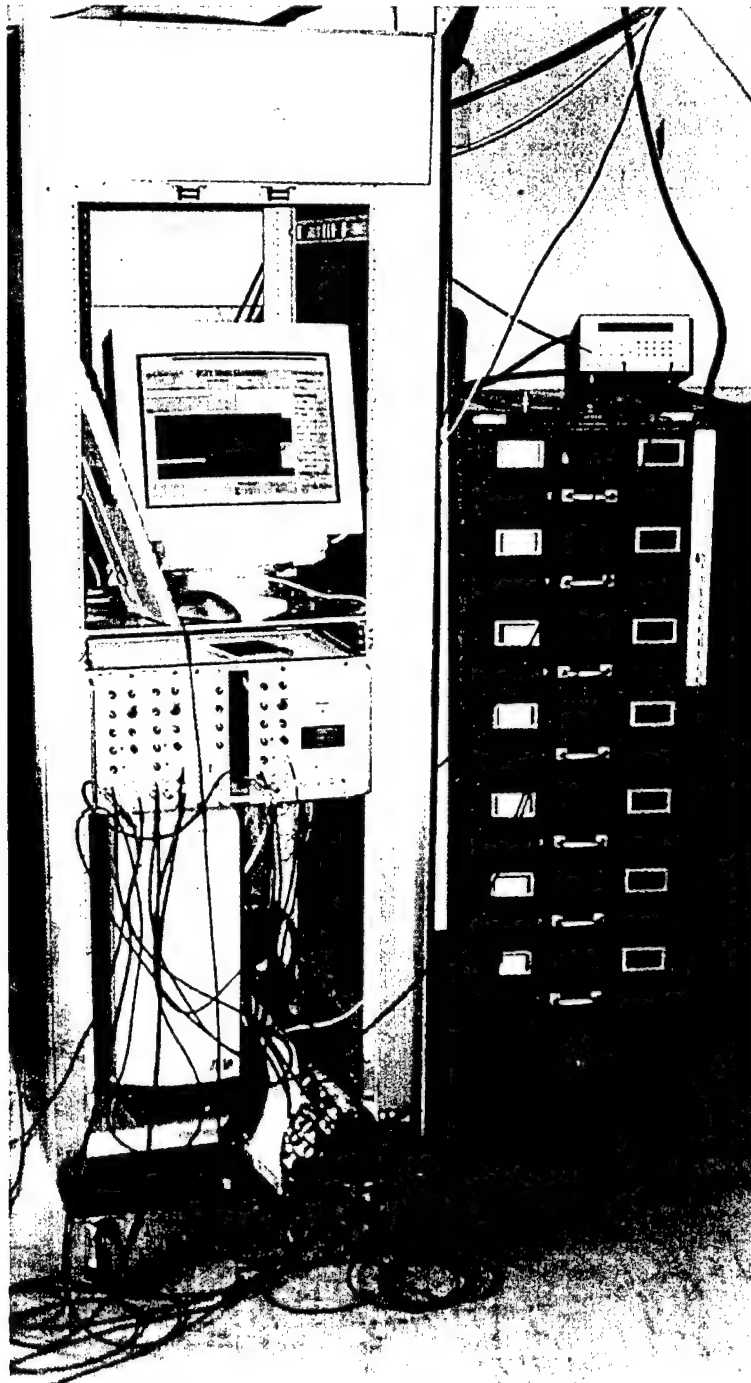


Figure 33. DGV Computer and Control Rack

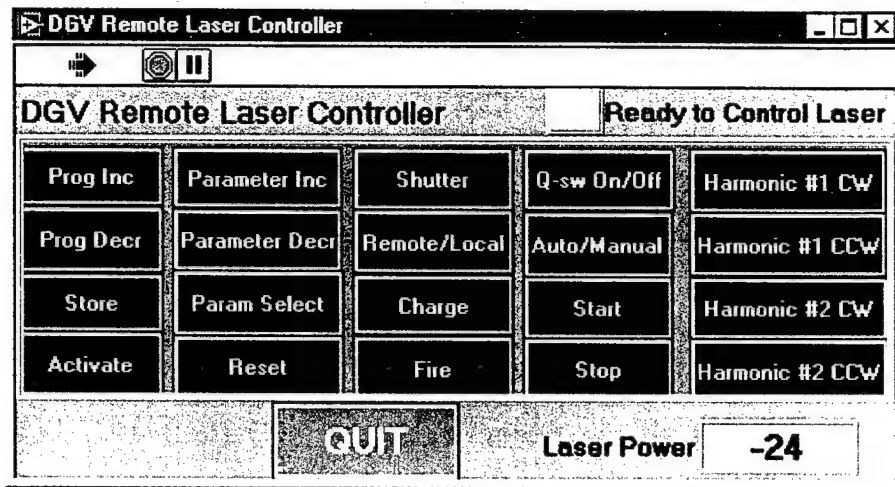


Figure 34. DGV Remote Laser Controller Screen

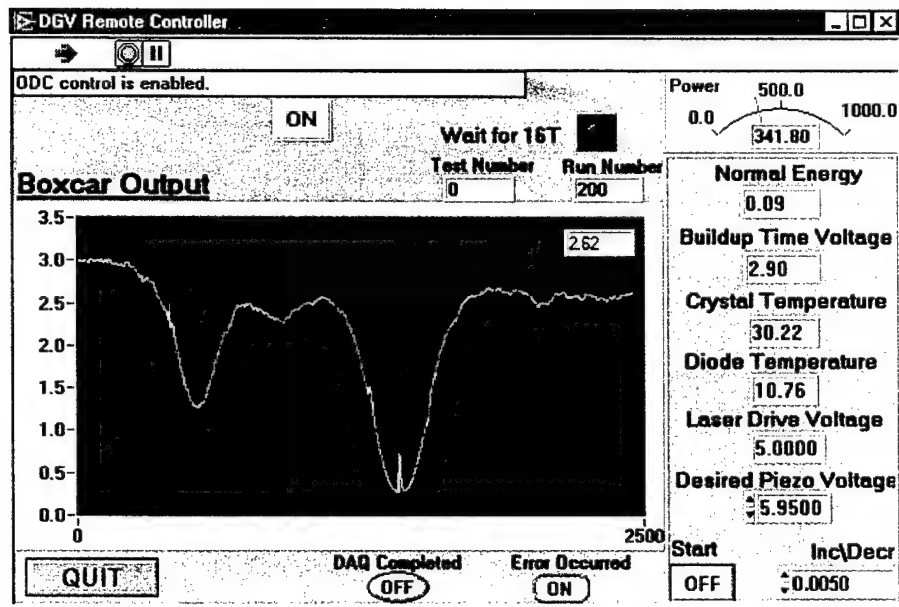


Figure 35. Remote Tuning of the DGV Laser Frequency

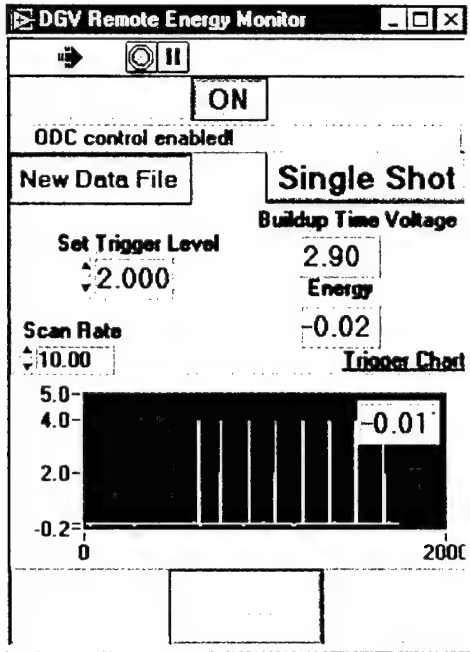


Figure 36. DGV Remote Energy Monitor

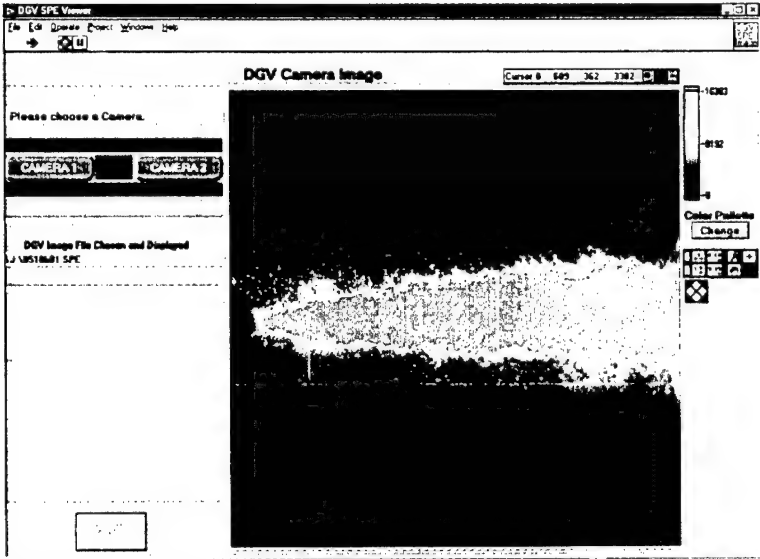


Figure 37. DGV Image Viewer on the ODC

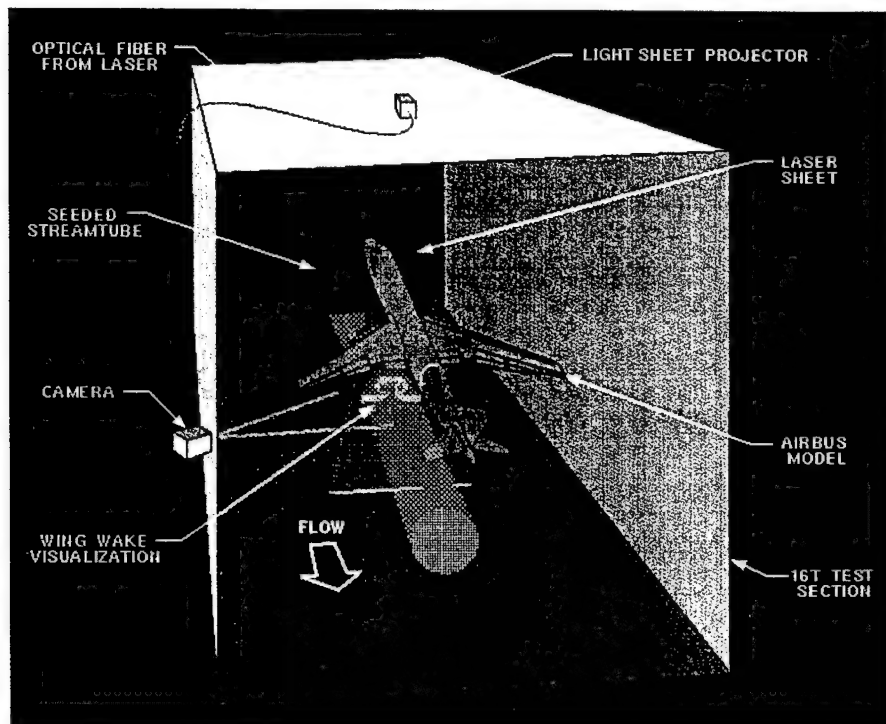


Figure 38. Concept of the Laser Vapor Screen Installation

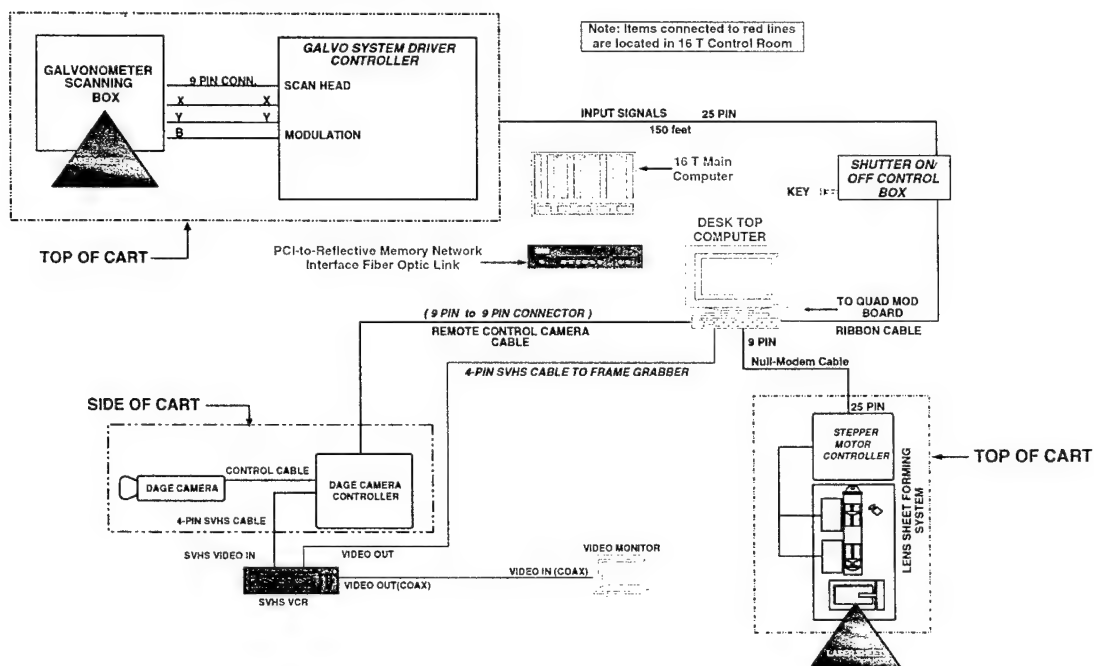


Figure 39. Schematic of the LVS Hardware



Figure 40. Effect of Axial Position

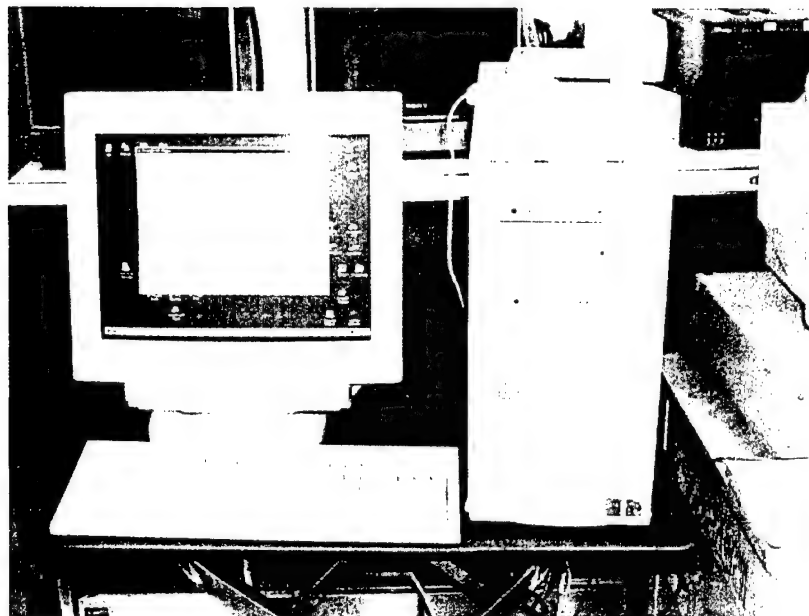
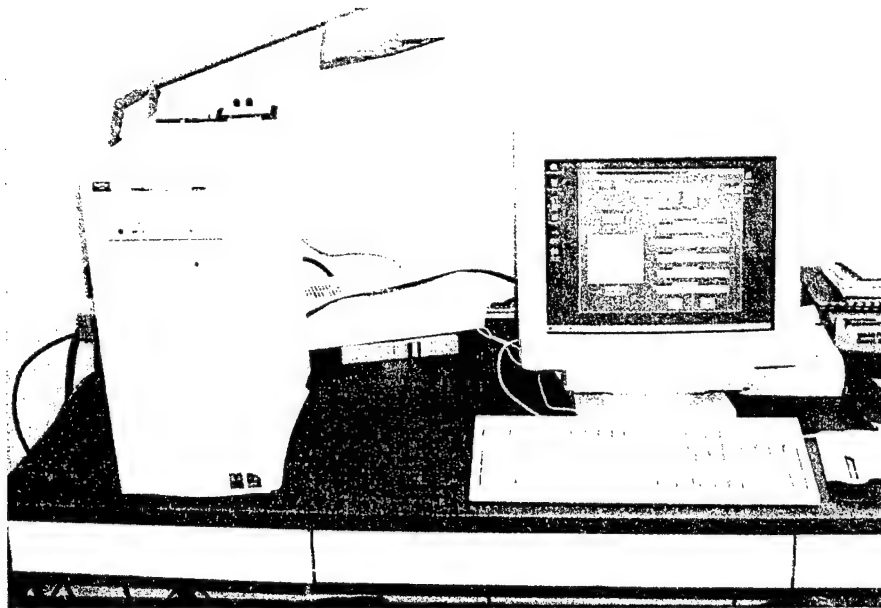
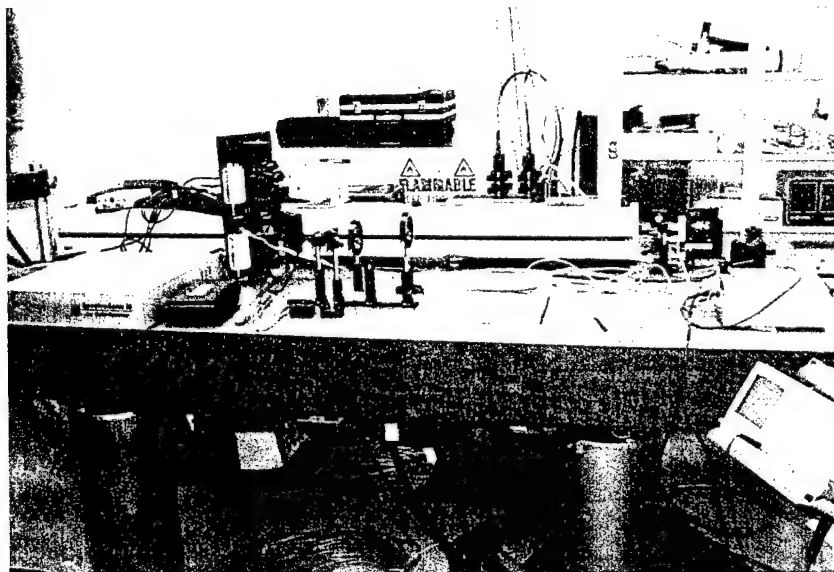


Figure 41. ODC Setup for LVS Integration Demonstration



**Figure 42. LVS PC Setup for LVS Integration Demonstration**



**Figure 43. LVS Laser and Hardware**



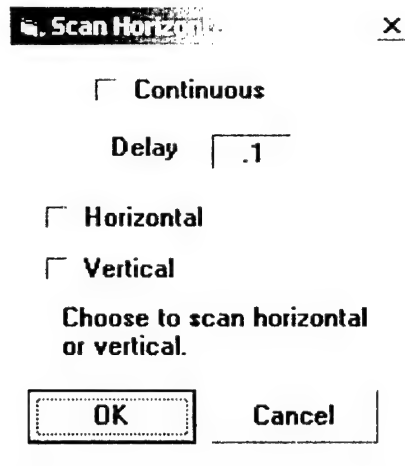


Figure 44. Screen from Program used for LVS  
Scan Control from the LVS PC

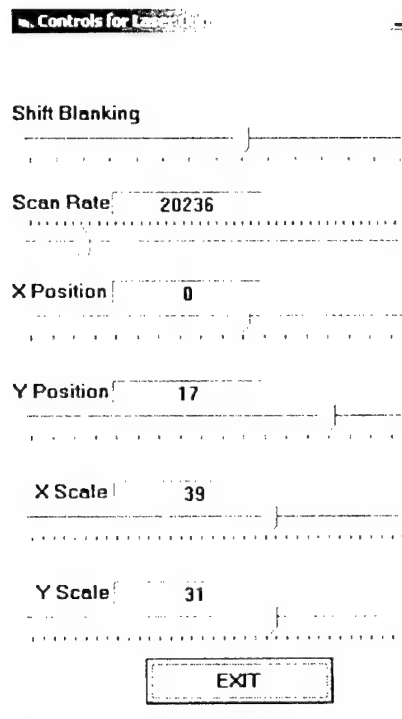


Figure 45. Screen from Program used for LVS  
Laser Control from the LVS PC

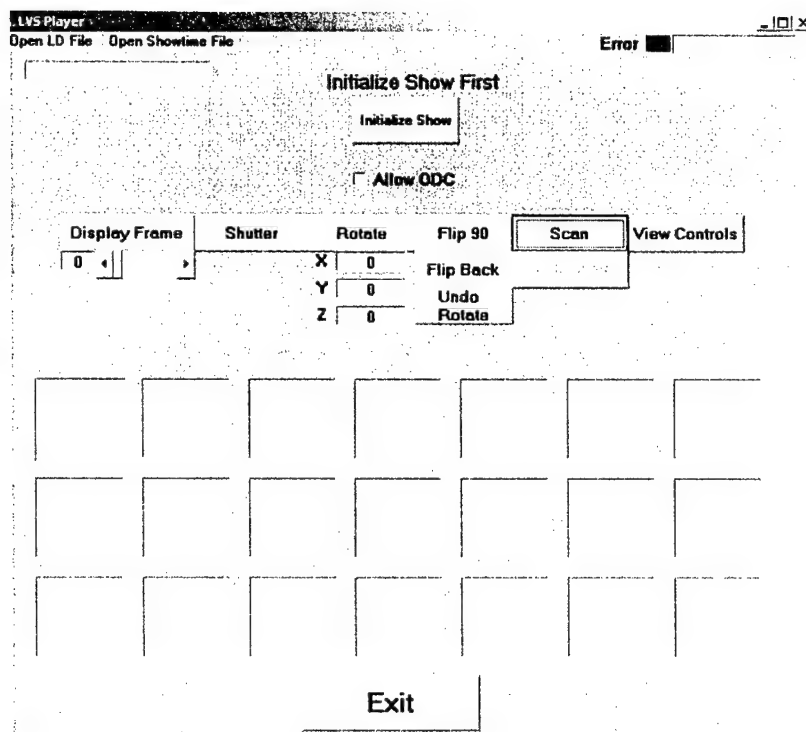


Figure 46. Screen from Program used for LVS Showtime Control from the LVS PC

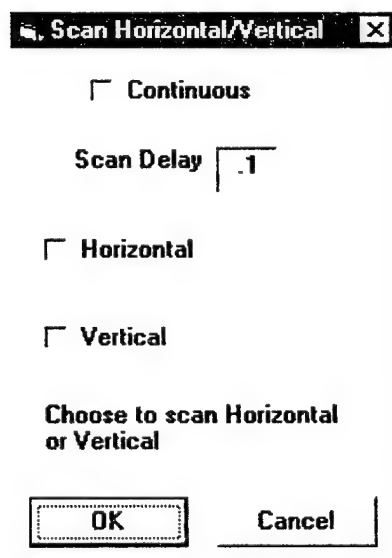


Figure 47. Screen from Program used for LVS Scan Control from the ODC PC

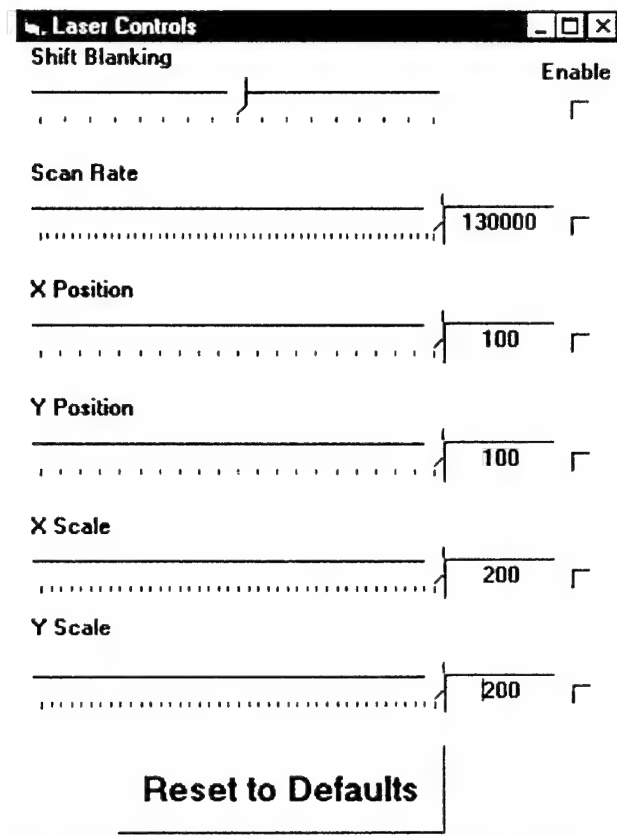


Figure 48. Screen from Program used for LVS Laser Control from the ODC PC

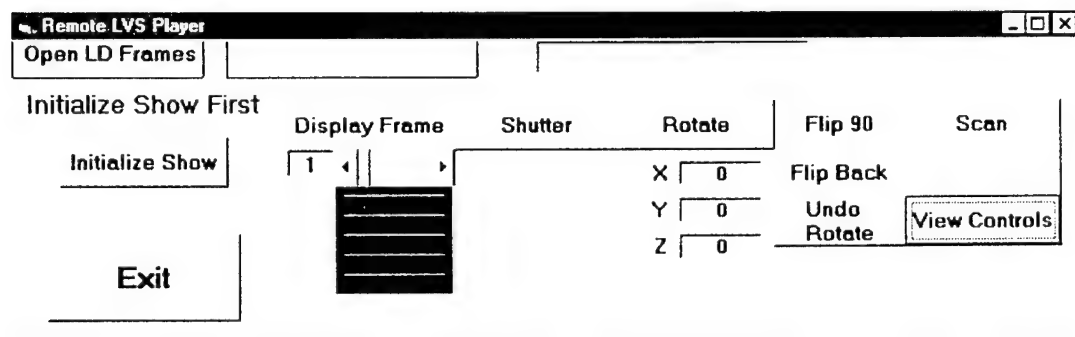
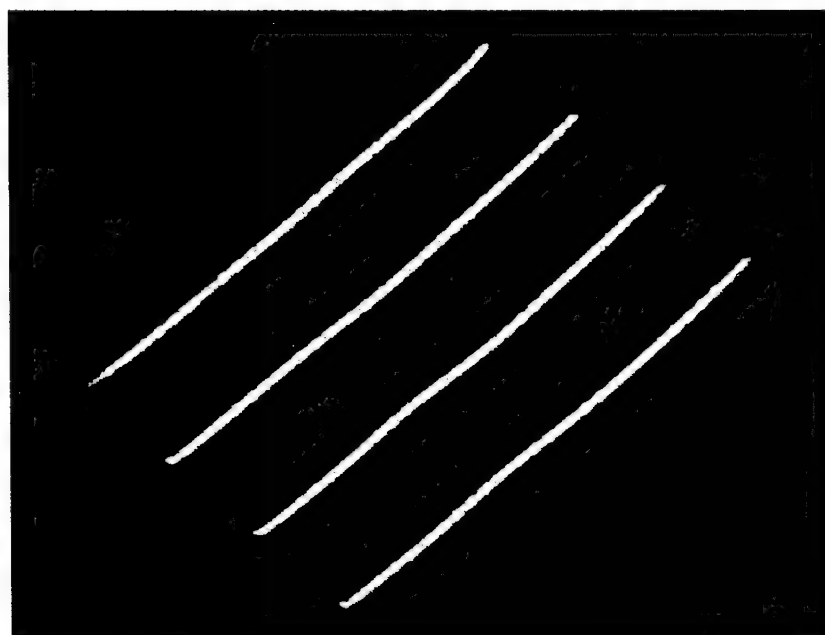


Figure 49. Screen from Program used for LVS Showtime Control from the ODC PC



**Figure 50. Horizontal Lines Screen**



**Figure 51. Screen of Lines at 45 deg**

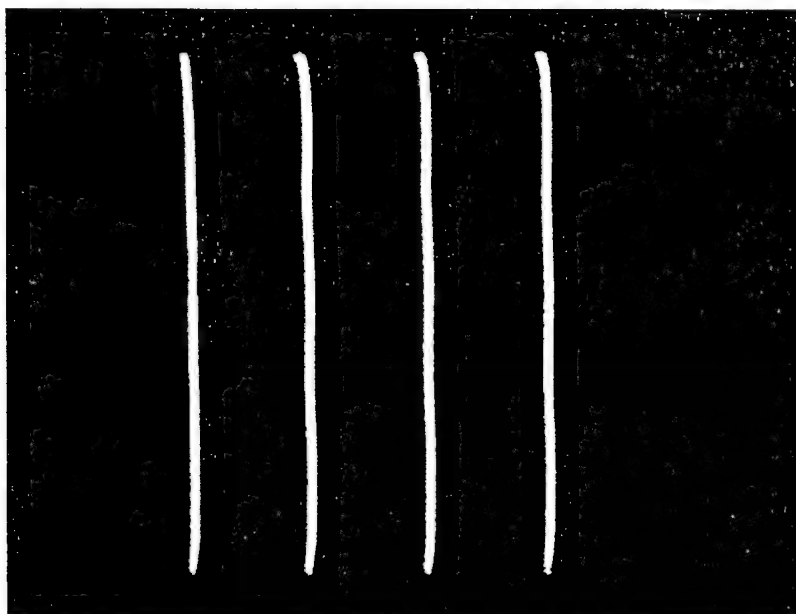


Figure 52. Vertical Lines Screen

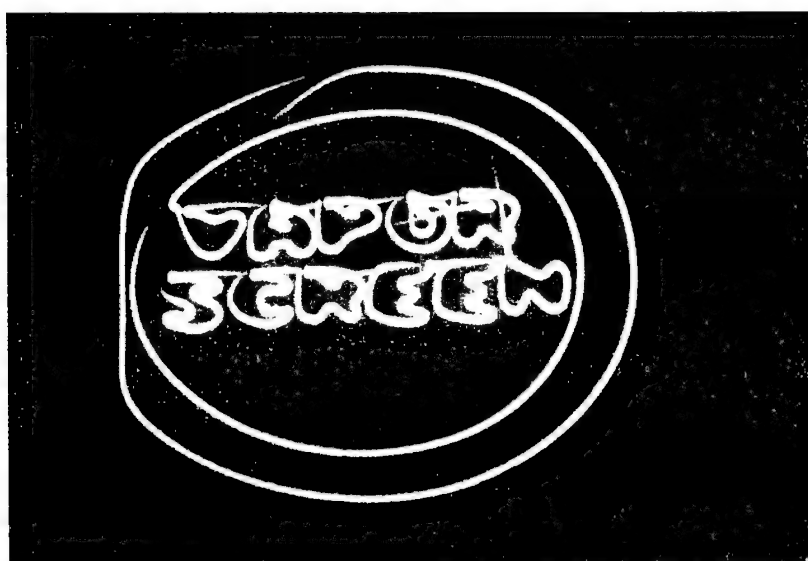
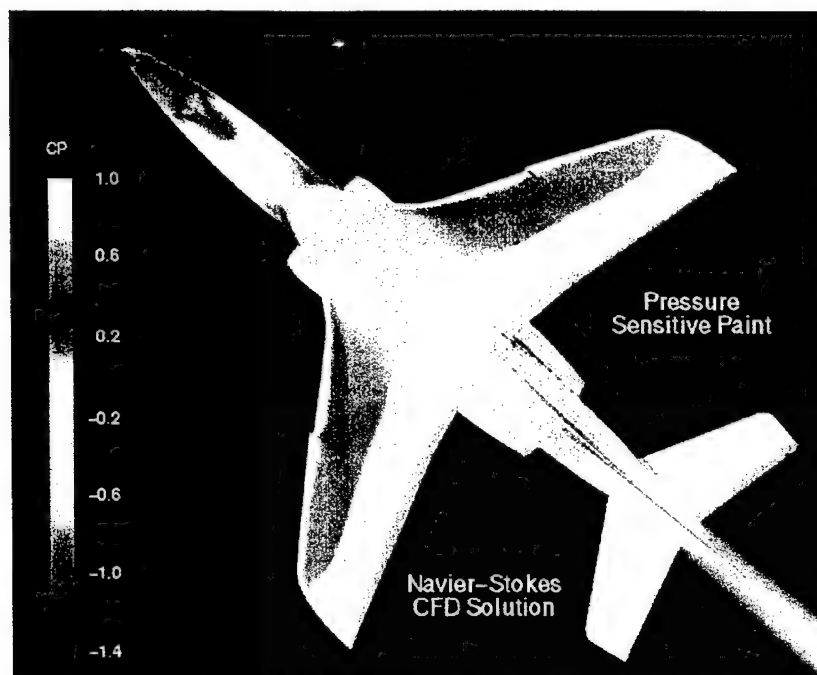
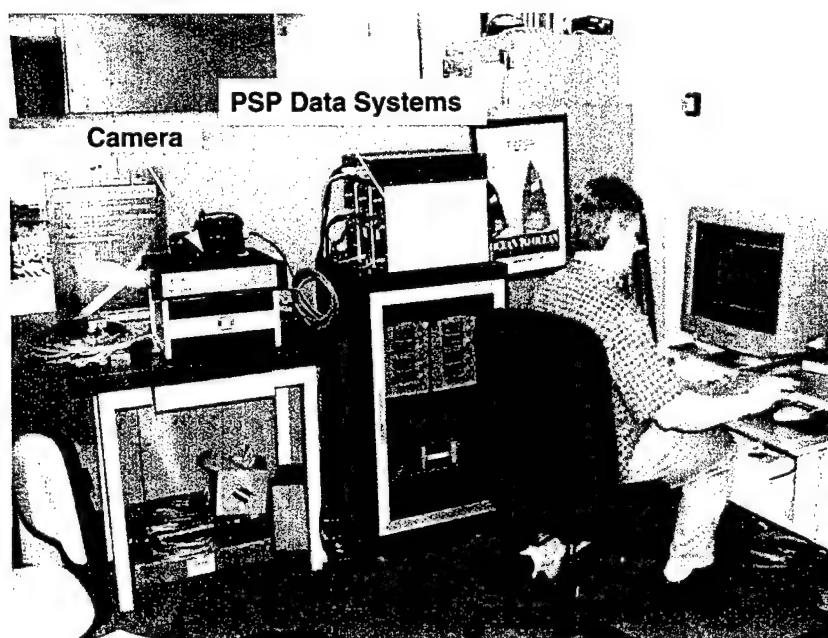


Figure 53. Vapor Screen Logo



**Figure 54. Example of Comparison between PSP Data and CFD Calculations**



**Figure 55. PSP Image Annotation Demonstration Hardware**

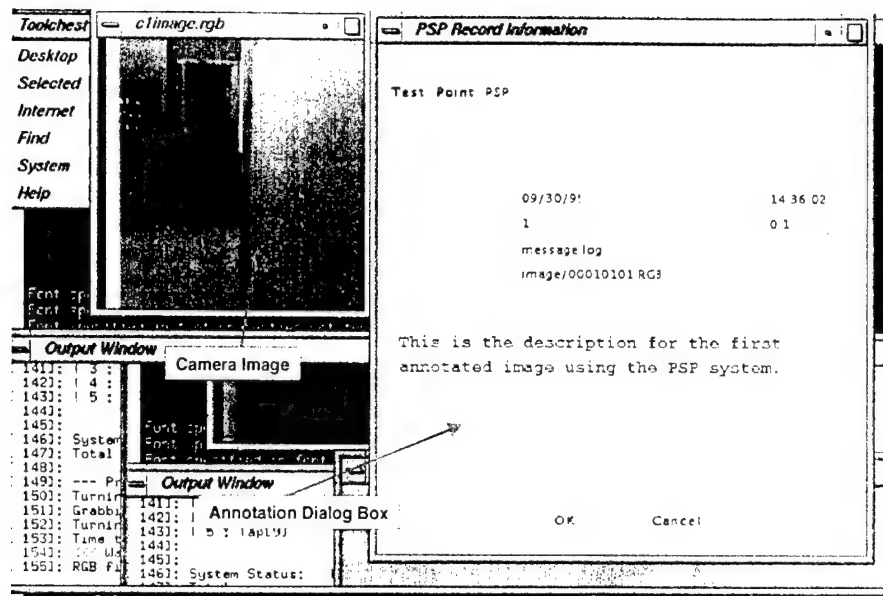


Figure 56. Unix Screen of PSP Image Annotation Process

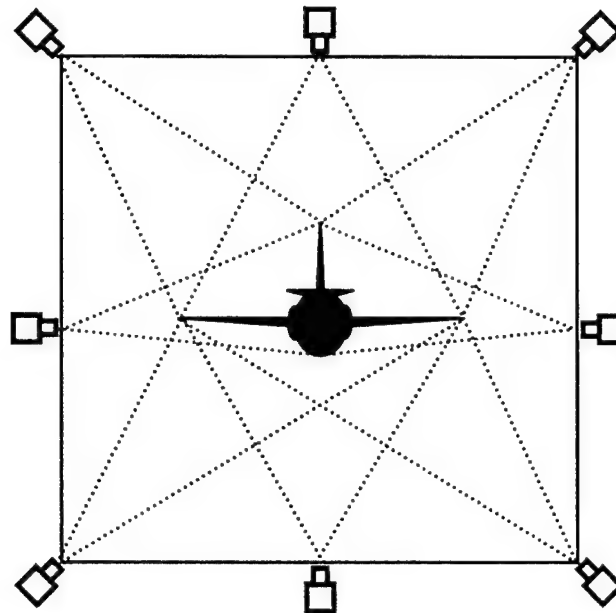


Figure 57. Schematic of Eight-Camera PSP System for the 16T Wind Tunnel

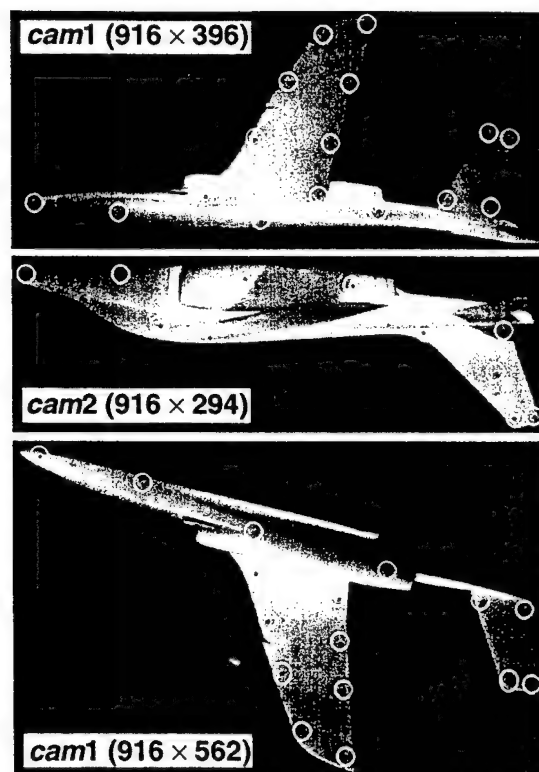


Figure 58. Circles Indicating Registration Markers Used in Analysis of PSP Images

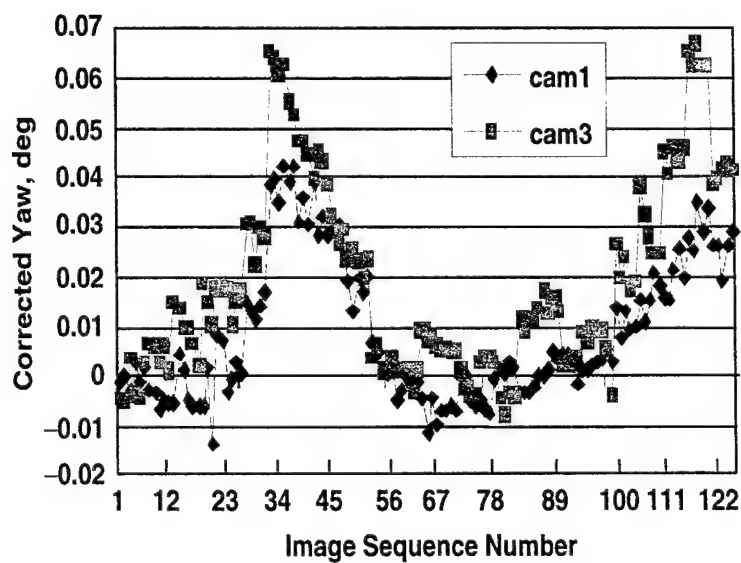


Figure 59. Yaw Angles from PSP Image Data



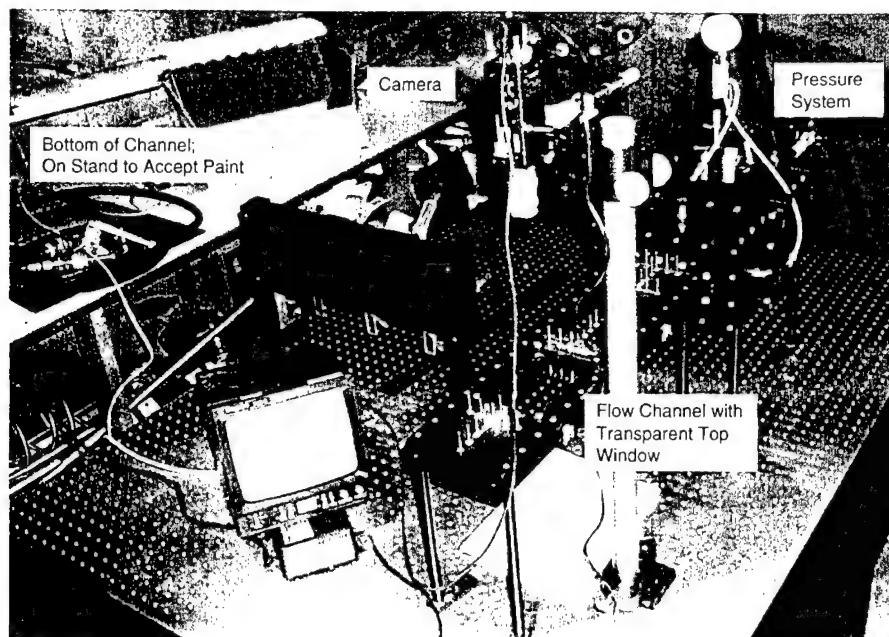


Figure 60. Shear Stress Experimental Configuration

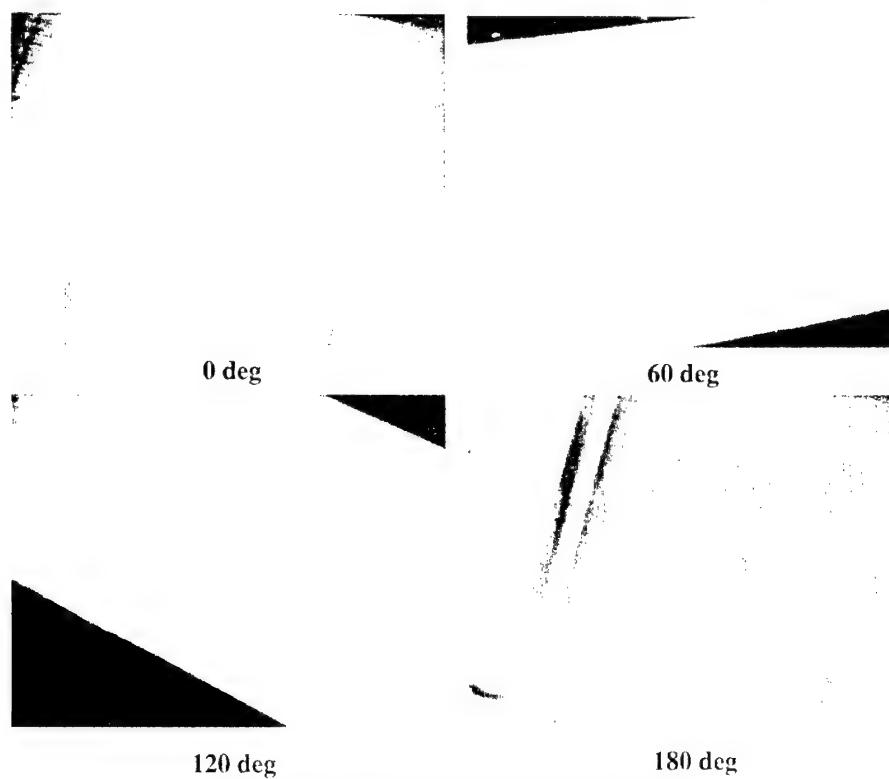


Figure 61. Shear Stress Data Images

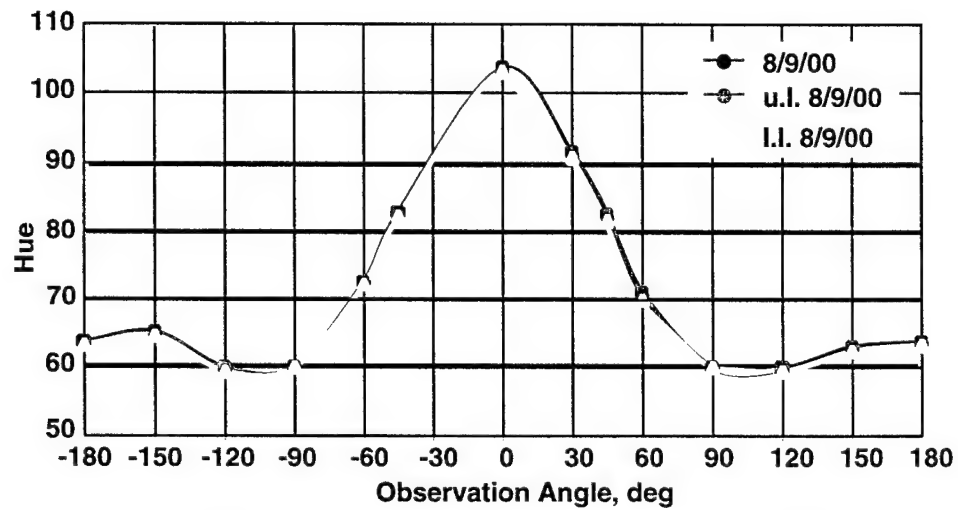


Figure 62. Shear Stress Data: Hue versus Observation Angle

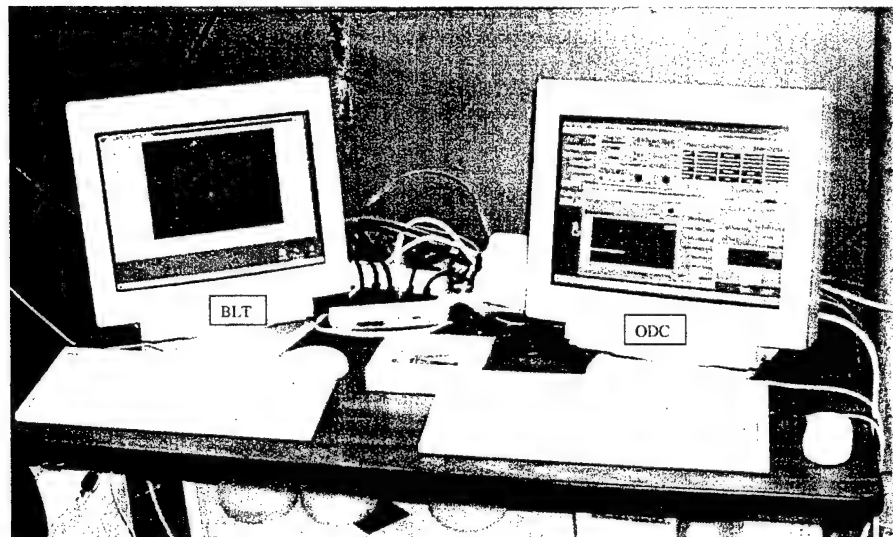


Figure 63. ODC and BLT Computers

**16T Interface for ...**

Parameters Received from 16T

Time Elapsed for DAQ  
0 mins 5.918 secs

Send Number DAQ Complete  
5

Run Number  
200

Test Article  
DGV

Error Status

File to VMIC

ODC Port ODC IP Address  
6556 134.137.99.72

16T Port 16T IP Address  
6557 134.137.26.246

Figure 64. 16T Interface for Data Transfer (Sustainment)

**Read 16T Tunnel Data**

File Edit Operate Project Windows Help

Data Retrieved Successfully

Input Run Number Run Number Not Found Run Number

File to VMIC

Input Test Article Test Article

Error Status

Figure 65. 16T Interface for Data Transfer ( Nonsustainment)

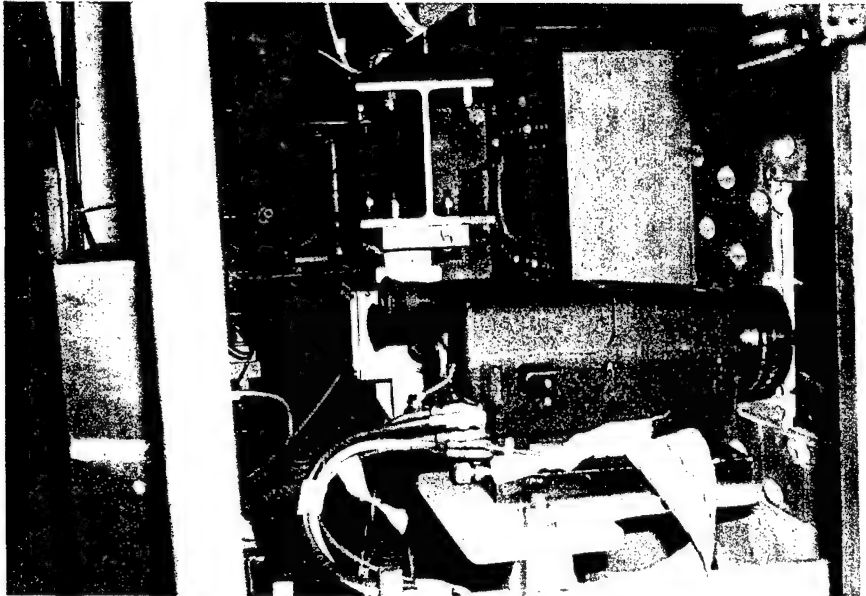


**Figure 66. BLT Installation in 16T**

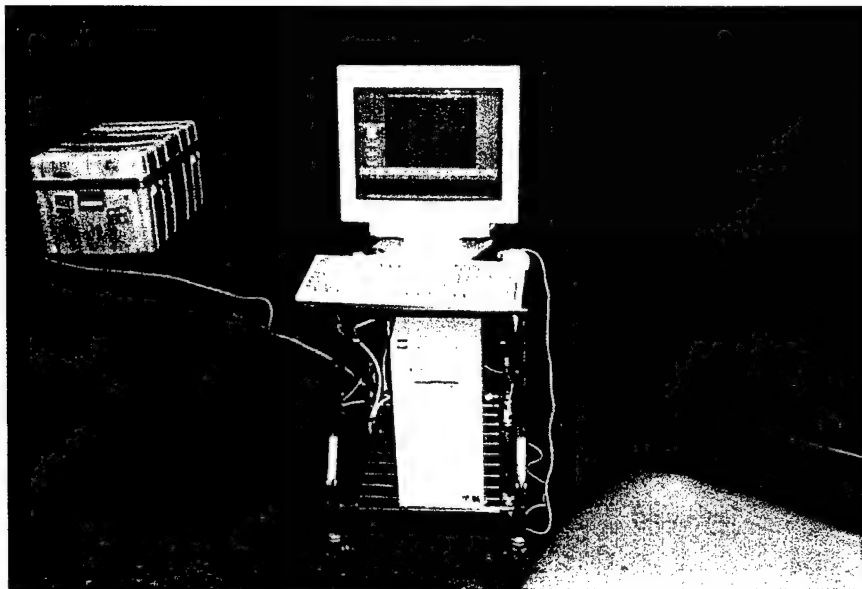


**Figure 67. BLT PC Placement in 16T**

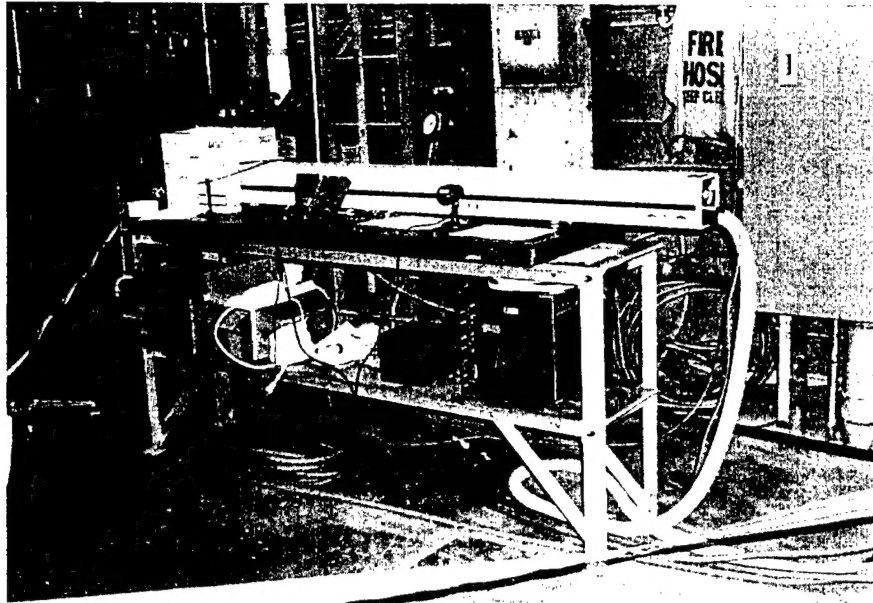


Figure 68. LVS Laser Installation in 16T

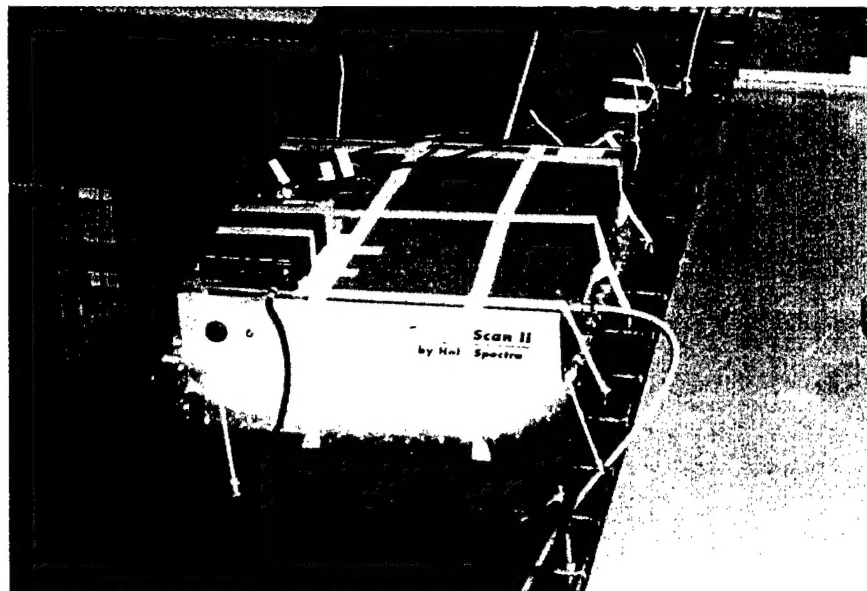
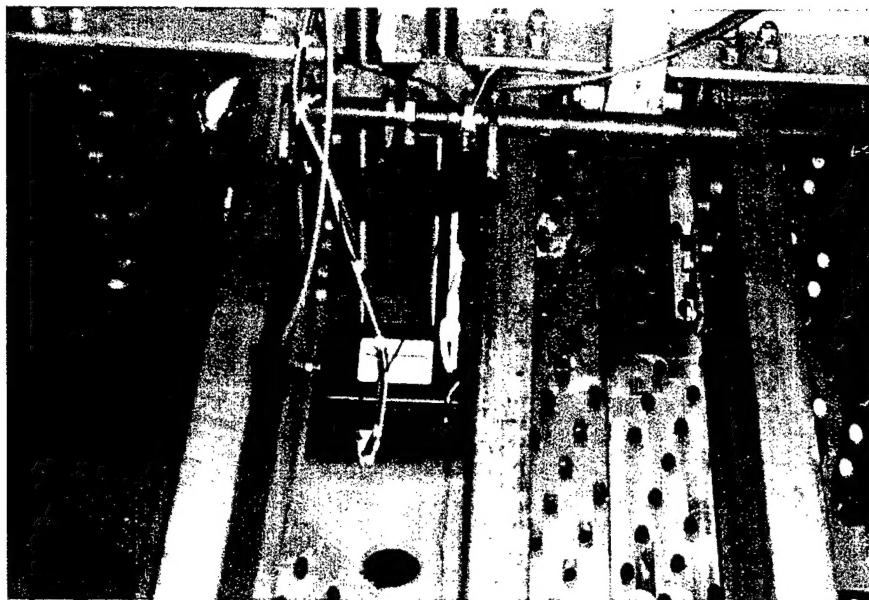
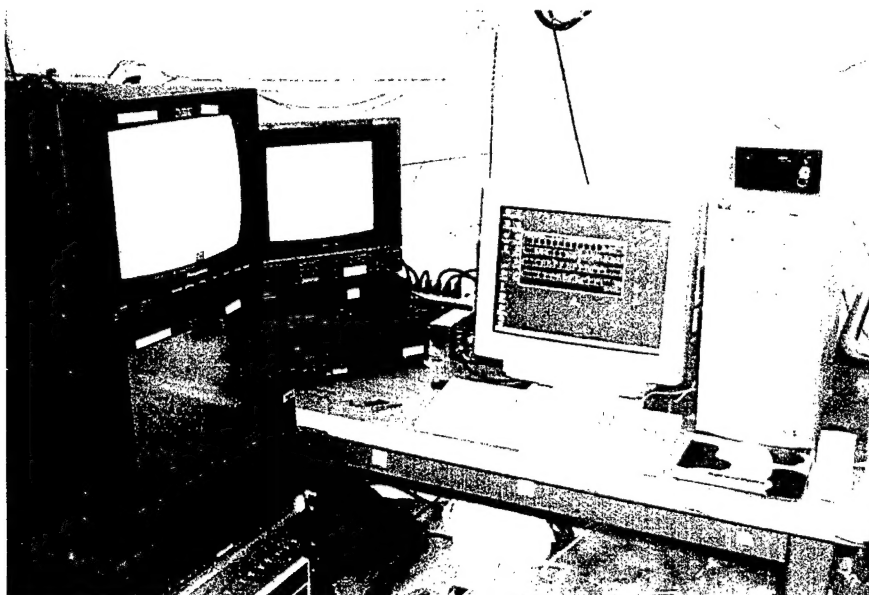


Figure 69. LVS Controller Installation in 16T



**Figure 70. LVS Galvanometer Installed in 16T**



**Figure 71. LVS PC Setup in 16T**



Figure 72. ODC Setup in 16T

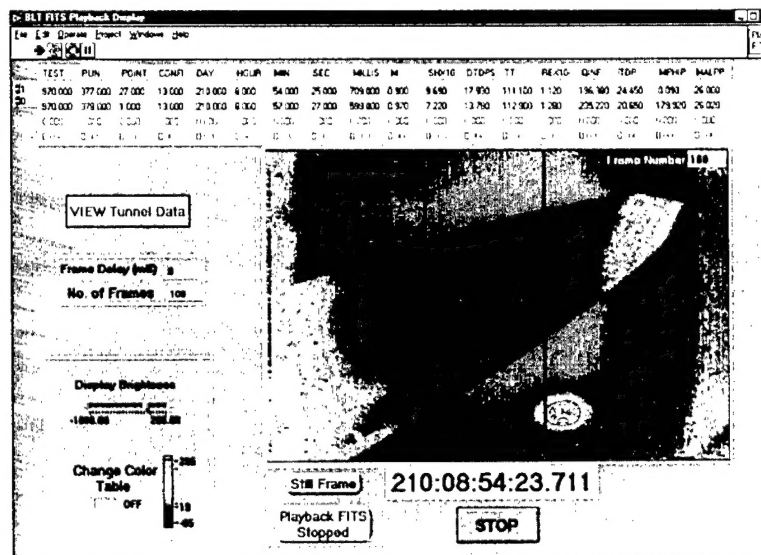


Figure 73. BLT 16T CTS Test Data Taken Showing Tunnel Conditions on 7/28/00

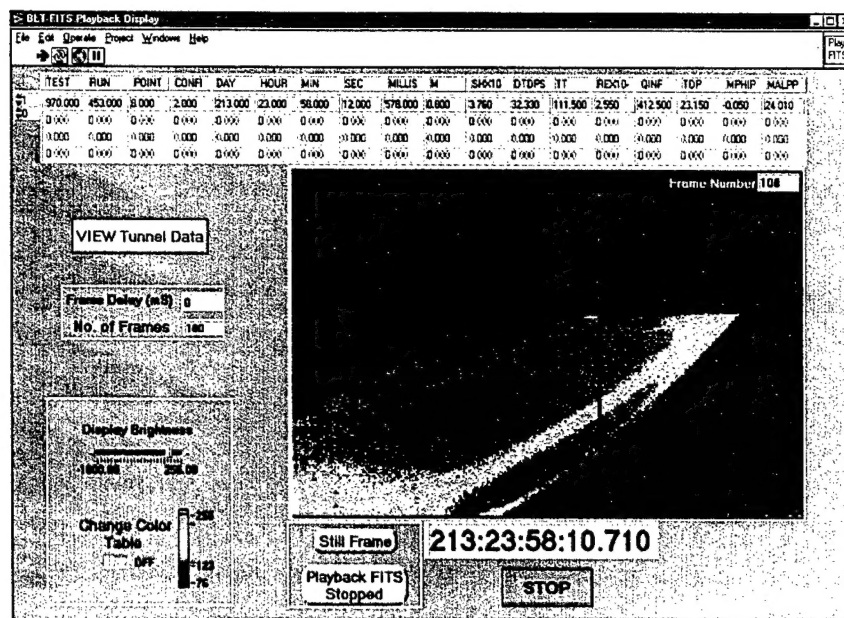


Figure 74. BLT 16T CTS Test Data Taken Showing Tunnel Conditions on 7/31/00

Table 1. Schedule of Deliverables for the ODS Program

Deliverable			Completed
Optical Diagnostics Controller	M1		7/30/99
PSP Image Enhancements for Archives	M2		9/30/99
Demonstrate PSP Annotation		D1	9/30/99
Laser-Based FLOW Visualization	M3		5/31/00
Model Deformation and Positioning	M4		9/5/99
Boundary-Layer Transition Detection	M5		2/24/00
Demonstrate ODC Integration in Lab		D2	9/30/99
Shear Stress and Skin Friction	M6		not mature
Doppler Global Velocimetry Integration	M7		9/30/99
DGV and BLT Integration	M8		5/19/00
Demonstrate Diagnostic Integration in 16T		D3	8/1/00
Project Plan Revision			10/22/99
Technical Report			9/30/00